Engineering Failure Analysis 170 (2025) 109310

Contents lists available at ScienceDirect

Engineering Failure Analysis

journal homepage: www.elsevier.com/locate/engfailanal

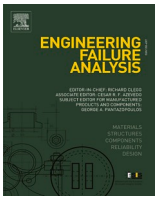

Automatic detection of local collapse mechanisms in historical masonry buildings: Fast and robust FE upper bound limit analysis☆

Martina Buzzetti *, Natalia Pingaro, Gabriele Milani [1]

Politecnico di Milano, Department of Architecture, Built Environment and Construction Engineering, Piazza Leonardo da Vinci 32, 20133 Milan, Italy

ARTICLE INFO

Keywords:
Masonry structures
Limit analysis
No-tension material
Local failure mechanisms
Failure analysis under horizontal loads

ABSTRACT

A fast and robust FE upper bound limit analysis approach is proposed, aimed at predicting the spectral acceleration that triggers local failure mechanisms on historical masonry constructions. Structural verifications are made in agreement with the Italian building code, without assuming pre-assigned local failure mechanisms and with masonry unable to withstand tensile stresses. Structural elements are discretized through infinitely resistant hexahedrons coupled with quadrilateral interfaces obeying a Mohr-Coulomb failure criterion and where all plastic deformation is lumped. Two different horizontal load distributions are investigated, namely constant and reverse linear along the height. Several different in-plane directions of the seismic entrance are considered. The kinematic limit analysis problem, written in its standard form, is solved using a consolidated linear programming routine. In function of the tensile strength, the collapse acceleration and the active failure mechanism are found automatically. Through iterative extrapolation, the results for the no-tension material model are deduced. Finally, a novel filtering algorithm is proposed that considers active exclusively the elements belonging to the failure mechanism, thus allowing the estimation of the spectral acceleration responsible for the collapse. The procedure is applied on two complex historical buildings located in northern Italy.

1. Introduction

Most of the built heritage of many European and Mediterranean countries characterized by a moderate and high seismic hazard, such as Italy, Greece, Slovenia, Albania, Morocco, and Turkey, is constituted by unreinforced masonry buildings [1]. Historical masonry structures were generally designed to withstand only vertical loads, and in many cases, they exhibit ineffective connections between perpendicular walls, roofs, and floors. Consequently, when subjected to horizontal forces (such as those induced by an earthquake), they are unable to activate a box behavior, but rather local collapse mechanisms are triggered. Sometimes, the high slenderness (defined for masonry as the height-to-thickness ratio) of some façades is responsible for out-of-plane failures even if effective connections are present [2]. This is the reason why, after strong earthquakes, the overturning of single walls and the

☆ This article is part of a special issue entitled: 'Failure of masonry' published in Engineering Failure Analysis.

* Corresponding author.
E-mail address: martina.buzzetti@polimi.it (M. Buzzetti).

[1] The author Gabriele Milani is an editor of this journal. In accordance with policy, Gabriele Milani was blinded to the entire peer review process.

https://doi.org/10.1016/j.engfailanal.2025.109310
Received 21 October 2024; Received in revised form 23 December 2024; Accepted 12 January 2025
Available online 13 January 2025

appearance of mechanisms involving the roto-translation of large portions of façades failing in bending [3–9] are observed.

Hence, the detection of out-of-plane failures is paramount for both historical heritage preservation and life. The first studies on the out-of-plane behavior of masonry walls probably date back to Rondelet [10], who framed the problem in terms of stability. Subsequently, Limit Analysis approaches were proposed, starting from Heyman's seminal work [11]. Limit analysis, which is a force-based approach where external loads are applied statically, can be computed using either the static theorem, providing a lower-bound multiplier of the collapse load, or the kinematic one, by leading to an upper-bound solution. The actual collapse load multiplier is determined by that solution that satisfies the hypotheses of both theorems: equilibrium, compatibility, plastic strain flow rule and material admissibility. Typically, the kinematic theorem is much more straightforward, because intuitively simpler. Furthermore, it can be used either manually with a single Lagrangian variable of motion on pre-assigned failure mechanisms, or combined with Finite Elements FEs, as it will be discussed later. In the manual approach, to solve the problem, the principle of virtual works can be adopted by selecting a mechanism before setting a certain distribution of loads (including the self-weight and the horizontal accelerations) and compatible generalized virtual displacements. The collapse acceleration is then computed by equating the work expended by the horizontal loads to that by the "stabilizing" forces, mainly gravity, having assumed masonry as unable to withstand tensile stresses and assuming that the failure mechanism is constituted exclusively by macro-blocks linked by flexural hinges were dissipation is null. In a conventional safety assessment, the failure mechanism is not triggered if the multiplier of the horizontal loads is higher than the expected acceleration demand. In other words, the seismic acceleration that activates such kind of local failures can be found directly from the collapse multiplier computed using limit analysis. The ultimate acceleration so evaluated should be then compared with the code one, estimated for the site where the building is located. If the latter is higher, the structure is unsafe, and strengthening is needed.

Limit analysis is traditionally used in the literature [12–16] for the safety assessment of existing buildings characterized by the activation of partial failure mechanisms. Assuming for masonry an ultimate behavior where its limited tensile strength is neglected (no-tension material hypothesis), on the safe side predictions of the ultimate load-carrying capacity can be provided, at the same time excluding from the computations that extra-resistance induced by the energy dissipation needed to open those crack patterns forming the failure mechanism. When dealing with complex geometries and to realistically detail the interaction among piers, spandrels, vaults, and slabs, limit analysis must be necessarily combined with FEs. In the literature, there are already many dedicated non-commercial codes [17–25]. They are based mainly on the kinematic theorem, but also static approaches have been proposed. Both exhibit relevant drawbacks, for instance, the upper bound approach is straightforward, but unfortunately, an overestimation of the load-carrying capacity (not on the safe side) is possible. On the contrary, the static theorem provides lower-bound failure multipliers, but is very unpractical, especially in the case of 3D massive structures, since boundary conditions should be imposed on stresses [26].

For existing buildings, the Italian code, in parallel with global analyses [27,28], requires investigating the possible activation of partial out-of-plane collapses employing the so-called "linear kinematic analysis", which is a one-degree-of-freedom limit analysis on pre-assigned mechanisms where masonry is assumed unable to withstand tensile stresses. The user is thus called to work manually on simplified geometries and easy mechanisms, which in most cases are classic and trivially based on the formation of horizontal hinges (mode I failure). Following this approach, the behavior of each macro-element is studied independently from the other portions of the structure. Therefore, the collapse mechanism is evaluated by considering a kinematic chain of rigid bodies and attributing the dynamic characteristics of a single-degree-of-freedom system. Although this method is very simple and fast, the effective collapse mechanism is strongly dependent on the geometry and the construction details. Hence, the actual behavior might be remarkably different from that of the simplified model adopted. Typically, several crucial features such as the interconnection between perpendicular walls are arbitrarily assigned and left to the user's discretion. Furthermore, other phenomena are disregarded, such as sliding and crumbling. Moreover, the intrinsic discontinuity of masonry is neglected since the approach assumes rigid blocks, but it is well known that masonry behaves as an assemblage of elements that interact, and especially when subjected to seismic actions, they are also free to separate and sometimes slide, at least locally.

Being in such a problem crucial a precise detailing work on the geometry and on the distribution of the vertical loads, typically existing software puts at disposal plugins for the local analyses, which work on models that are unlinked from those used for the non-linear static analyses, which typically are carried out on FE models of the entire buildings.

From previous considerations, it appears clear that the need to use limit analysis to identify those collapse mechanisms triggering in a seismic event is nowadays considered well-established practice. However, still today, the utilization of displacement-based global non-linear approaches (i.e. considering the entire structure) –no matter if a full 3D FE, an equivalent frame approach or a Distinct Element DE model are used- are considered the standard analyses to carry out [29–34], even for out-of-plane failures, since experimental tests have shown that unreinforced masonry walls may exhibit a certain post-cracking out-of-plane displacement capacity [2,30].

Global non-linear analyses exhibit some advantages, since they allow the study of (i) the global behavior as well as (ii) the activation of possible local failure mechanisms without selecting them a priori [35–41].

However, they are also characterized by some issues and difficulties that the interested technician must consider with particular care.

Generally speaking, it is notorious that masonry is quite stiff up to collapse and the adaptation to displacement-based design sounds to many researchers like a stretch. When full 3D FE meshes are used, sometimes the collapse mechanism cannot be correctly detected [42–44] because the discretization used is typically rough to maintain the computation burden acceptable. The detection of the ultimate displacement is not straightforward, because a scarcely resistant material model barely allows reproducing drops in the global pushover curve. Recently, in [45] there has been an attempt −based on energetic considerations- to provide an estimation of the ultimate displacements in non-linear static analyses in all those cases where the global pushover curve does not show any drop of the base shear applied. However, the method is indirect and "slow" nonlinear dynamic analyses are needed, a drawback that makes the

approach unsuitable for research and seismic assessments at professional level, where simplicity and efficacy should be preferred.

Moreover, when using FEs many parameters should be set and calibrated to define an adequate constitutive model for non-linear materials like masonry. For instance, the Concrete Damage Plasticity (CDP) model, which is probably the most used one, certainly in many cases proved to capture some basic features of the behavior near collapse [46–53], but at the cost of calibrating by trial and error many non-linear material parameters, some of them purely numerical, among the others the most important being the viscosity parameter. Indeed, the smaller it is, the more accurate the output. However, the computational burden increases exponentially when the viscosity parameter drops down and there is a higher frequency of premature halting for lack of convergence. When dealing with historical masonry, the matter becomes even more intricate, because of the presence of pre-existing cracks and the absence of the necessary experimental information to determine the mechanical properties of masonry.

Some of the issues arising from the adoption of the CDP model could be avoided using FE models with interface elements, which also allows a sliding failure beside failures in tension and compression. However, their application is generally limited to micro modelling and therefore to small case-studies, such as walls, arches, vaults and domes [54–56].

FE models are also employed to perform non-linear dynamic analyses [49,57,58], that proved to be more realistic than pushover. However, the computational time required generally precludes their usage in common practice, and the results are strongly influenced by the accelerogram selected in input.

Considering such crucial limitations, an alternative is the use of the Distinct Element Method DEM. Since collapses of individual portions of the structure are mainly governed by the presence of rigid blocks and well-defined crack patterns, such an approach seems to be the most appropriate one, as it catches the intrinsic masonry nature [59–63].

Because DEM is native heterogeneous, the analysis of large-scale structures is always associated to prohibitive computational burden.

Typically, time-history analyses are carried out applying artificial or real accelerograms. It is quite common, therefore, that numerical results in DEM show significant variability, induced by the chosen input accelerations/velocities fields. DEM is therefore computationally demanding also because of this. Furthermore, it is worth noting that its application in a static fashion is typically obtained in dynamics, applying a slow velocity/acceleration ramp at the base [45,64]. Consequently, pushover is also computationally demanding, and commercial software itself is costly.

Another noteworthy method for nonlinear seismic analyses is the so-called Applied Element Method AEM [65–67]. AEM is a numerical approach conceived to predict both the continuum and discrete behavior of structures. It employs a modeling technique based on discrete cracking, enabling it to automatically track structural collapse behavior through all loading stages: elastic response, crack initiation and propagation in tension-weak materials, reinforcement yielding, element separation, element contact, and collision, as well as impacts with the ground or adjacent structures. Nevertheless, AEM models present several limitations. One major issue is the high computational burden, especially for complex structures. Indeed, the subdivision of the structure into small elements with detailed interactions significantly increases computation time. Additionally, the accuracy of AEM analyses relies heavily on the quality of the constitutive models used to represent the materials. For advanced or heterogeneous materials, such as composites (like masonry), or reinforced structures, the available models may either be inadequate or require extensive calibration. Another challenge is related to the precise calibration of material parameters and element interactions, a process that can be complex and often dependent on experimental data, which are not always at disposal. Moreover, while AEM excels in simulating progressive collapse and failure, it may not be the most efficient for ordinary static analyses or cases where a high resolution of the collapse modes is not required. The method is also highly sensitive to the geometric accuracy of the model, and the complexity of its outputs can make result interpretation challenging for engineers who are not specialized in this field.

A further alternative to previously discussed methods is to adopt some geometry simplifications, as occurs in the equivalent frames. When equivalent frames are used, masonry piers and spandrels are modeled by means of “equivalent” non-linear beam elements connected by rigid links. The failure mechanism activating in such analyses is usually global. Typically, partial out-of-plane mechanisms −like the corner failure or the combined in- and out-of-plane collapse- elude such modelling strategy without being identified, despite a partial mitigation to such major drawback has been attempted by [68], who implemented a new element −conceived for the utilization in equivalent frames- where out-of-plane collapses may occur. However, still the major simplifications adopted on the geometry do not allow a realistic reproduction of the actual failure occurring, at least for historical buildings with high complexity. Furthermore, the model is intrinsically unable to deal with curved masonry elements, or it appears artificial for churches or towers, i.e. when a clear identification of piers and spandrels is not straightforward.

Another problem common to all global strategies is the evaluation of the interlocking between perpendicular walls. Sensitivity analyses should be carried out, but the computational effort is unreasonable. Considering all the previous issues, limit analysis appears the only method immediately attractive for the common user, because with a single step numerical simulation, an estimation of the collapse acceleration can be found in a reasonably rapid way, allowing to carry out sensitivity analyses and −if used in association with FEs- being able to identify automatically partial mechanisms, in case the behavior of the building is local.

Some attempts have been presented in the specialized literature, basing both the kinematic and static variants of the theorems, ideally coupling limit analysis with a FE discretization of the domain [69–72].

In the present work, a numerical approach belonging to the family of limit analysis coupled with FEs [26,73] is presented and applied to assess the structural safety of complex historical masonry palaces when subjected to seismic actions. The principal aim is the verification of the out-of-plane local mechanisms, following the prescriptions provided by Italian standards, but at the same time avoiding the above-mentioned drawbacks. The proposed code −developed in-house within the software MATLAB- is based on the methodology proposed in [26]. In particular, masonry is discretized through infinitely resistant hexahedrons coupled with quadrilateral interfaces obeying a Mohr-Coulomb failure criterion, where all plastic deformation is lumped. The kinematic limit analysis

problem, written in its standard form, is solved by means of linear programming, deriving automatically in post-processing collapse loads and active failure mechanisms, at the same time providing by an iterative extrapolation also the results under the no-tension material assumption, as mandatorily requested by the Italian building code. Such an iterative approach is needed to avoid numerical issues when dealing with a material unable to withstand tensile stresses. From the collapse acceleration and the failure mechanism so retrieved, an effective filtering algorithm −which is the main novelty of the paper- is proposed. It considers an element active if and only if its horizontal velocity exceeds a lower bound threshold, set in input by the user to exclude those parts of the structure that do not participate in the activation of the mechanism in a significant manner. Solving such a crucial issue, it is possible to estimate the spectral acceleration that is associated with the activation of the local failure mechanism.

The limit analysis-based approach implemented by the authors is fast, needs only the definition of the geometry (in the same way done by a common FE software), of the loads, and of the strength criterion. Finally, the selection of pre-assigned failure mechanisms is not required. The approach proposed is discussed in detail in Section 2 and benchmarked in Section 3. In Section 4 practical applications are presented. In particular, two quite complex palaces located in northern Italy, the so-called Vittorio Emanuele II palace (Case Study 1) and the former monastery of Santa Maria della Pace (Case Study 2) are analyzed. Computations are carried out only on significant portions of such structures, which are characterized by a peculiar geometry and are the most vulnerable ones. The results in terms of collapse acceleration, active failure mechanism, and safety verification are finally discussed in Section 5.

2. Numerical approach for the identification of local failure mechanisms

A numerical approach based on the upper bound limit analysis coupled with FEs is presented for the assessment of existing/historical masonry structures where out-of-plane failures are the most common. The methodology proposed is in accordance with Italian standards [27,28] but has the advantage that it does not require the selection of pre-assigned mechanisms. According to [26], a classic limit analysis problem can be formulated for any masonry structure if the following assumptions are made: (i) the structure is discretized with infinitely resistant hexahedron elements, as shown in Fig. 1 and (ii) interfaces −where inelastic deformations are lumped- are considered rigid-perfectly plastic with infinite ductility. In solving a standard limit analysis problem, the collapse load and the

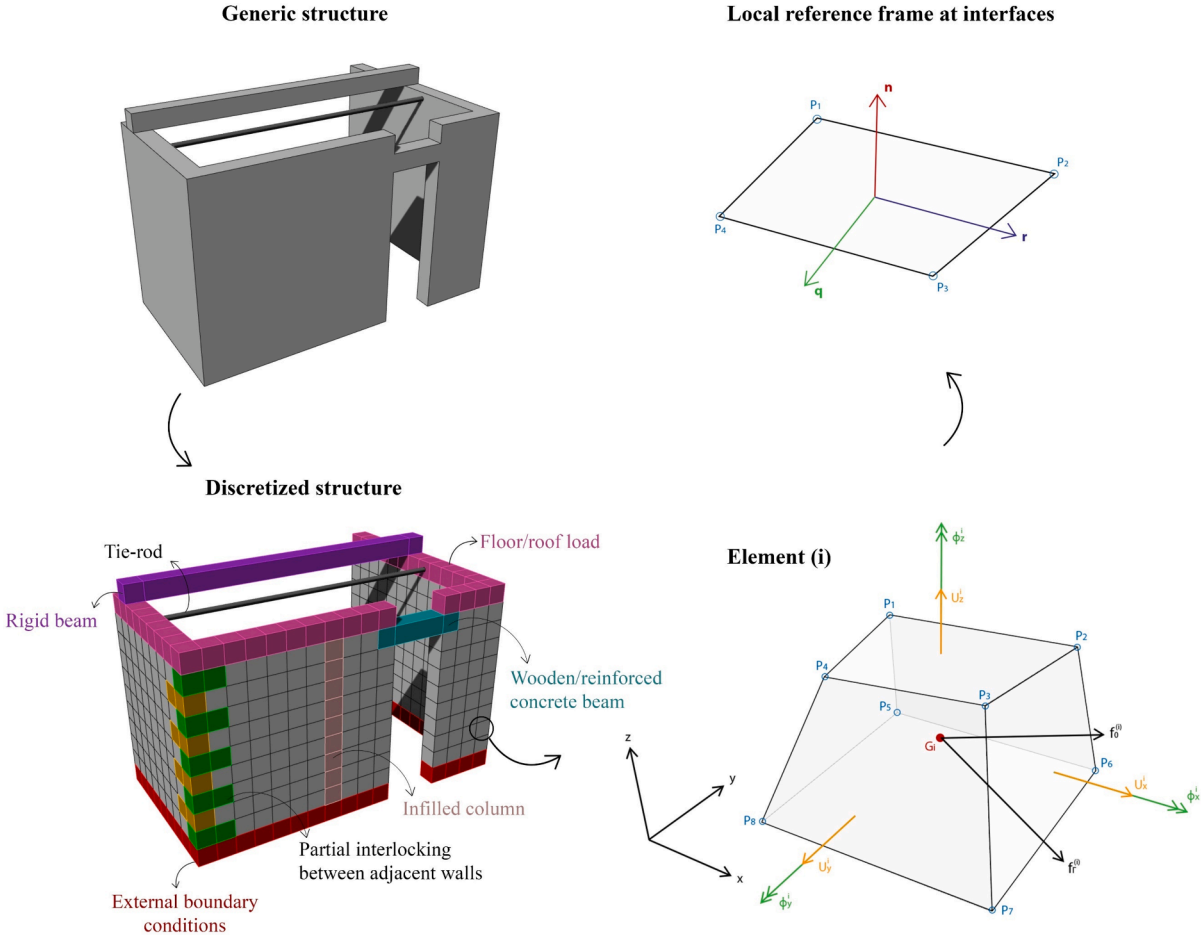

Fig. 1. Masonry structure discretization, generic Element (i) and interface local reference frame.

active failure mechanism are identified.

The formulated limit analysis problem can be stated either following the kinematic or the static theorems. According to the previous hypotheses, the material exhibits plasticity at a finite number of interfaces, meaning that the upper and lower bounds coincide. According to such deduction, the kinematic approach is used here since it is more straightforward, while the static counterpart may be in principle derived from the formulation of the self-dual linear programming problem.

The primal variables of the kinematic problem are six unknows per hexahedron, as depicted in Fig. 1: the centroid velocities along the reference axes (U_x^i, U_y^i, U_z^i) and the rotation rates around the centroid ($\phi_x^i, \phi_y^i, \phi_z^i$). Only external volume forces, dependent ($f_\Lambda^{(i)}$) or independent ($f_0^{(i)}$) on the load multiplier Λ, are assumed. In particular $f_0^{(i)}$ are gravity loads, while $f_\Lambda^{(i)}$ are horizontal forces mimicking seismic actions. In general agreement with the Italian building code [27,28], two horizontal load distributions are considered for $f_\Lambda^{(i)}$, namely G1 which is the so-called principal distribution of forces, proportional to the mass and linearly proportional to the height of the structure (inverted triangle distribution), and G2 −named as secondary distribution of forces-, proportional to the mass and uniform along the height of the construction.

Plastic compatibility is imposed constraining the jump of velocities at element interfaces since plastic dissipation is allowed only there. Being the interface quadrilateral, compatibility constraints are imposed on a faceted approximation of the actual surface constituted by four triangles with vertex in common located on the centroid, Then, four collocation points located at the vertices of the quadrilateral interface are considered, in which internal actions (obtained by multiplying the tangential and normal stresses by the triangle area), jump of velocities, and power dissipation are evaluated according to a suitable local reference frame. In this regard, the tern $\boldsymbol{n}-\boldsymbol{q}-\boldsymbol{r}$ identifies the local reference frame as shown in Fig. 1, where $\boldsymbol{n}$ is the unitary vector perpendicular to the interface, $\boldsymbol{r}$ is the unitary vector parallel to the edge defined by vertices P1 and P2, and $\boldsymbol{q}$ is perpendicular to both $\boldsymbol{n}$ and $\boldsymbol{r}$.

Therefore, the velocity at the collocation point CP_k belonging to element (i) in the local reference frame is evaluated as:

$$\boldsymbol{U}_{CPk}^{(i)} = \begin{bmatrix} \boldsymbol{n}^T \\ \boldsymbol{q}^T \\ \boldsymbol{r}^T \end{bmatrix} \begin{bmatrix} 1 & 0 & 0 & 0 & z_{Pk}-z_{G_{Ei}} & -\left(y_{Pk}-y_{G_{Ei}}\right) \\ 0 & 1 & 0 & -\left(z_{Pk}-z_{G_{Ei}}\right) & 0 & x_{Pk}-x_{G_{Ei}} \\ 0 & 0 & 1 & y_{Pk}-y_{G_{Ei}} & -\left(x_{Pk}-x_{G_{Ei}}\right) & 0 \end{bmatrix} \begin{bmatrix} \boldsymbol{U}^{(i)} \\ \boldsymbol{\phi}^{(i)} \end{bmatrix} = \boldsymbol{R}^{(i)}\boldsymbol{u}^{(i)} \tag{1}$$

$$\boldsymbol{U}^{(i)} = \begin{bmatrix} U_x^i & U_y^i & U_z^i \end{bmatrix}^T \tag{2}$$

$$\boldsymbol{\phi}^{(i)} = \begin{bmatrix} \phi_x^i & \phi_y^i & \phi_z^i \end{bmatrix}^T \tag{3}$$

Where: x_{Pk}, y_{Pk}, z_{Pk} are the collocation point CP_k coordinates, $x_{G_{Ei}}, y_{G_{Ei}}, z_{G_{Ei}}$ are the coordinates element (i) centroid.

Considering two adjacent elements (i) and (j) and assuming $\boldsymbol{n}$ as the outward vector from the element (i), the jump of velocities for the collocation point CP_k is equal to:

$$\Delta\boldsymbol{U}_{CP_k} = \boldsymbol{R}^{(j)}\boldsymbol{u}^{(j)} - \boldsymbol{R}^{(i)}\boldsymbol{u}^{(i)} \tag{4}$$

The proposed approach allows considering the presence of different structural materials and different properties at element interfaces, as highlighted with different colours in Fig. 1 in the discretized structure. The interfaces between adjoining elements are characterized by a Mohr-Coulomb failure criterion with tension and compression cut-offs, defined by tensile strength f_t, a compressive strength f_c, a cohesion c and a friction angle Φ.

The relation adopted between tensile strength and cohesion needs a dedicated short discussion.

Indeed, in the simulations, it is assumed that cohesion equates to tensile strength. According to consolidated literature [74,75], the utilization of a pure Mohr-Coulomb failure criterion, because of the moderate friction angles typically assumed for masonry (20-30°), is not recommended, since it would be responsible for an unrealistic too high ratio between tensile and tangential strength. Furthermore, in incremental analyses the presence of a tip in the strength domain may generate significant numerical issues, which justifies in general the utilization of either smooth strength domains or frictional failure criteria combined with a tension cutoff where the flow rule imposes a mode I crack propagation. On the other hand, speaking about the iterative procedure proposed for the first time by [73], which will be briefly recalled hereafter, it is carried out progressively reducing the tensile strength keeping constant the initial ratio between tensile strength and cohesion (hence also the latter drops to zero). The collapse acceleration of a structure is therefore estimated when f_t and c are contemporarily zero. When the failure mechanism is predominantly triggered by joints failing for the activation of the tension cutoff, a selection of a different $f_t/\ c$ ratio would lead in any case to the same results. In presence of some parasite sliding −always present for complex structures-, the previous statement is not rigorously true anymore, but if the failure mechanism remains predominantly flexural, authors experienced again the independence of the collapse multiplier upon $f_t/\ c$ ratio.

Returning back to the limit analysis model, in the local reference frame $\boldsymbol{n}-\boldsymbol{q}-\boldsymbol{r}$, the Mohr-Coulomb failure criterion with tension and compression cutoffs can be linearized leading to a set of linear inequalities describing the plastically admissible strength domain:

$$\boldsymbol{A}_{in}^I \begin{bmatrix} N_I \\ Q_I \\ R_I \end{bmatrix} \leq \boldsymbol{b}_{in}^I \tag{5}$$

where: $N_I = A_I\sigma_I, Q_I = A_I\tau_{q_I}, R_I = A\tau_{rI}$ are the internal actions, $\sigma_I, \tau_{q_I}, \tau_{rI}$ are the stress components acting along $\boldsymbol{n}$, $\boldsymbol{q}$ and $\boldsymbol{r}$, respectively,

A_I is the interface area.

Since an associate flow rule is assumed, the jump of velocities between adjacent elements (i) and (j) is linked with the plastic strain rate vector $\dot{\lambda}_I$, which is non-negative:

$$\boldsymbol{R}^{(j)}\boldsymbol{u}^{(j)} - \boldsymbol{R}^{(i)}\boldsymbol{u}^{(i)} - \boldsymbol{A}_{in}^{I\,T}\dot{\lambda}_I = 0 \tag{6}$$

$$\dot{\lambda}_I \geq 0 \forall I = 1, \cdots, N_{in} \tag{7}$$

Where N_{in} is the number of interfaces.

The power expended by the external volume forces is equal to:

$$P_0 = \sum_{i=1}^{N_e} V_i \boldsymbol{f}_0^{(i)\,T} \boldsymbol{U}^{(i)} \tag{8}$$

$$P_\Lambda = \Lambda \sum_{i=1}^{N_e} V_i \boldsymbol{f}_1^{(i)\,T} \boldsymbol{U}^{(i)} \tag{9}$$

Naming N_e the number of elements and V_i the volume of the i-th element.

As in any upper bound limit analysis, one failure mechanism can be identified among the infinite set of homothetic collapse deformed shapes defining the normalization condition, which is typically imposed assuming that the power dissipated by the loads depends on the load multiplier Λ is unitary when $\Lambda = 1$:

$$P_1 = \sum_{i=1}^{N_e} V_i \boldsymbol{f}_1^{(i)\,T} \boldsymbol{U}^{(i)} = 1 \tag{10}$$

The load multiplier is obtained from the balance of powers dissipated by internal and external forces (Eq. (8)) combined with the normalization condition (Eq. (10)):

$$\Lambda = \sum_{I=1}^{N_{in}} \boldsymbol{b}_{in}^{I\,T} \dot{\lambda}_I - \sum_{i=1}^{N_e} V_i \boldsymbol{f}_0^{(i)\,T} \boldsymbol{U}^{(i)} \tag{11}$$

According to the upper bound theorem, Eq. (11) is the objective function to minimize.

Finally, external boundary conditions can be defined with additional linear equalities. They are modelled as velocity constraints for those elements whose nodes are externally constrained, which are highlighted in red in Fig. 1:

$$\boldsymbol{A}_{bc}^{(h)} \boldsymbol{U}^{(h)} = 0 \tag{12}$$

where (h) represents the elements externally constrained and the number of rows of the matrix $\boldsymbol{A}_{bc}^{(h)}$ varies depending on the type of constraint.

Therefore, the limit analysis problem is defined as follows:

$$min\left\{ \Lambda = \sum_{I=1}^{N_{in}} \boldsymbol{b}_{in}^{I\,T} \dot{\lambda}_I - \sum_{i=1}^{N_e} V_i \boldsymbol{f}_0^{(i)\,T} \boldsymbol{U}^{(i)} \right\} \tag{13}$$

$$s.t. \begin{cases} \boldsymbol{R}^{(j)}\boldsymbol{u}^{(j)} - \boldsymbol{R}^{(i)}\boldsymbol{u}^{(i)} - \boldsymbol{A}_{in}^{I\,T}\dot{\lambda}_I = 0 \forall I = 1, \cdots, N_{in} \\ \sum_{i=1}^{N_e} V_i \boldsymbol{f}_1^{(i)\,T} \boldsymbol{U}^{(i)} = 1 \\ \boldsymbol{A}_{bc}^{(h)} \boldsymbol{U}^{(h)} = 0 \forall h \in b.c. \\ \dot{\lambda}_I \geq 0 \forall I = 1, \cdots, N_{in} \end{cases} \tag{14}$$

The standard linear programming solver available in MATLAB is used to find the collapse multiplier and the failure mechanism active [26].

For what concerns the strength domain to adopt for masonry, it is worth noting that the use of a zero tensile strength model –i.e. the assumption of a no tension material- is a widely accepted approach in classic literature, see for instance [76–79]. Also, the Italian standards require evaluating the acceleration triggering the local failure mechanism considering a no-tension material. This notwithstanding, the importance of assuming for masonry a no-tension material goes far beyond the Italian regulation, and it could be affirmed, on the contrary, that the latter transposes a long trend of research characterized by approaches where one of the major

assumptions is that masonry is unable to withstand tensile stresses. On the other hand, the application of limit analysis in presence of a non-vanishing tensile strength would be associated to an overestimation of the load carrying capacity and, in turn, would make the application of limit analysis theorems debatable. Indeed, in tension masonry exhibits an elasto-fragile behavior, which violates one of the hypotheses of applicability of limit analysis, namely the perfectly plastic behavior with infinite ductility. As a major consequence, the resultant load carrying capacity would be overestimated, with predictions provided not on the safe side. The efforts spent towards the proposal of numerical strategies able to deal with limit analysis in presence of a no-tension material go in such direction.

However, enforcing the no-tension material hypothesis may be responsible for the activation of parasite sliding between contiguous elements or stalling issues of the numerical algorithm.

As a workaround, the iterative limit analysis originally proposed by [73] to provide failure loads in presence of no-tension material assumptions is adopted. The idea is based on the following two fundamental hypotheses, namely (i) that only a limited sliding between contiguous blocks is allowed and (ii) that the extrapolation of the results for no-tension material occurs assuming as reference a failure mechanism deemed not affected by undesired sliding induced by the too small tensile strength. Let us consider for the sake of example two solutions in the velocity field −say $\boldsymbol{U}_1^{(i)}$ and $\boldsymbol{U}_2^{(i)}$ − of the same limit analysis problem constituted by the same FE model, but with masonry characterized by a strength domain that is homothetically scaled passing from Solution #1 to Solution #2. Let us also make the hypothesis that the obtained failure mechanism does not change its shape, meaning that the velocity fields $\boldsymbol{U}_1^{(i)}$ and $\boldsymbol{U}_2^{(i)}$ are either identical or proportional. In particular, with reference to the normalization condition (Eq. (10)), it can be easily proved that such condition imposes that$\boldsymbol{U}_1^{(i)} = \boldsymbol{U}_2^{(i)}$. Plastic multipliers at the interfaces in the two solutions are also the same, meaning that the internal plastic dissipation decreases linearly with the shrinkage of the strength domain. On the contrary, power expended by gravity P_0 remains constant, because the velocities field does not change. From the previous considerations, the objective function $\sum_{I=1}^{N_{in}} \boldsymbol{b}_{in}^{I\,T} \dot{\lambda}_I - \sum_{i=1}^{N_e} V_i \boldsymbol{f}_0^{(i)\,T} \boldsymbol{U}^{(i)}$ is thus linear in f_t (or linear in any other mechanical parameter characterizing quantitatively the homothetic expansion or shrinkage of the strength domain). Remembering that the objective function is the collapse multiplier of the loads Λ (a relation deduced from power balance and normalization condition), and repeating limit analysis computations progressively reducing f_t, allows graphing Λ-f_t plots and at the same time identifying the active failure mechanisms. Λ-f_t graph is therefore linear in all those intervals of f_t where the same failure mechanism is triggered.

When f_t decreases, the numerical optimization becomes more and more difficult, albeit with a certain variability from case to case, the collapse multiplier tends rapidly to zero and spurious local sliding between contiguous blocks occurs, induced by the insufficient cohesion.

Furthermore, a predominant spurious sliding is theoretically responsible for an inapplicability of classic limit analysis concepts. In case of sliding, indeed, the flow rule is typically non-associated (in violation of limit analysis theorems) and this circumstance puts doubt on the accuracy of the predictions provided. From a practical point of view, with a zero-cohesion material, there may be some equilibrium problems even under the application of self-weight in all those elements (e.g. spandrels and openings in general) where vertical interfaces connect them to the rest of the structure, because the latter are initially subjected to low or absent normal precompression, with a consequent lack of resistance against sliding. A discussion about this important issue −and the reader is referred there for further details- can be found in [73], where a masonry portal is analyzed with benchmarking purposes.

Such last consideration showcases the importance of proposing an iterative approach able to deal “indirectly” with a material unable to withstand tensile stresses.

In turn, for many cases of technical interest, the activation of mechanisms with spurious sliding are usually associated to a negative failure acceleration extrapolated for a no tension material, which clearly demonstrates that the mechanism provided by limit analysis is unrealistic.

The relevance of sliding in the formation of a failure mechanism is quantitatively assessable computing the amount of internal power dissipated for tangential stresses, or more directly with a rapid visual inspection of the deformed shape at collapse. Bearing in mind the previous considerations, the determination of the most suitable mechanism to consider for the evaluation of the collapse acceleration by extrapolation is straightforward.

It is also interesting to point out that some sliding is frequently present and unavoidable in real assessments, because of the intrinsic complexity of the geometry. The extrapolation of the behavior of a specific structure at $f_t = 0$ can be therefore not strictly univocal, i.e. more than one failure mechanism could provide non-negative collapse accelerations. In case of non-univocality, the safest option should be always preferred.

It is also worth mentioning that the passage from limit analysis to a standard safety assessment (which is the main goal of the paper, i.e. to put at practitioners’ disposal an automatic plug-in to use in common design) needs special attention when the failure mechanism is local (as it occurs in most of the cases for buildings with insufficient stiffness of the floors and bad interlocking between perpendicular walls). Indeed, the activated mass is in this case much less than that found for a global analysis. Furthermore, amplifications are possible for mechanisms involving upper floors. When accounting for all the mass, this overestimates the actual capacity of the structure, a shortcoming that is in common with the assumption of pre-assigned failure mechanisms (as recommended by the Italian code). A filtering strategy is therefore needed to properly account for the activation of complex mechanisms not easily predictable in anticipation simply isolating portions of the structure assumed presumably critical.

The new plug-in proposed here is believed necessary to compute correctly the spectral acceleration. Referring to the Italian building code [27,28] −but any other code dealing with partial failure mechanisms can be used- the value of the seismic action that activates the failure mechanism corresponds to the spectral acceleration a_0^* evaluated as:

$$a_0^* = \frac{\alpha_0 \cdot g}{e^* \cdot FC} \tag{15}$$

Where α_0 is the collapse multiplier, g is the gravity acceleration, FC is the confidence factor and e^* is the fraction of participating mass defined as:

$$e^* = \frac{g \cdot M^*}{\sum_{i=1}^{n+m} P_i} \tag{16}$$

where $n+m$ is the number of self-weights P_i whose masses, due to the seismic action, generate horizontal forces on the elements of the kinematic chain. M^* is the participating mass computed as:

$$M^* = \frac{\left(\sum_{i=1}^{n+m} P_i \delta_{x,i}\right)^2}{g \cdot \sum_{i=1}^{n+m} P_i \delta_{x,i}^2} \tag{17}$$

where $\delta_{x,i}$ is the horizontal virtual displacement of the application point of the i-th weight P_i.

Within the FE limit analysis code here presented, the main aim of the novel filtering procedure proposed is to avoid the over-estimation of the spectral acceleration a_0^*, which is calculated in agreement with the Italian code, which implicitly considers only a small portion of the building interested by the activation of the failure mechanism. In particular, the participating mass M^* is computed considering only the elements of the structure having a displacement $\delta_{x,i}$ larger than a pre-established threshold (i.e. at least 10 % or 20 % of the maximum one). It is worth mentioning that the Italian standards erroneously label $\delta_{x,i}$ as displacements, that are velocities since the kinematic theorem of limit analysis is used.

Moreover, only a G2 distribution is assumed in the code for the calculation of the local mechanisms, which is a limitation for a FE approach, like the present one, that can model the entire structure or large portions of it. Hence, in the case of a G1 distribution, the collapse load α_0 in Eq. (15) is substituted by $a_g/g = \frac{base\ shear}{vertical\ load}$ to consider properly the actual distribution of forces applied to the structure.

In agreement with intuition, authors experienced applying the filter that the load carrying capacity (in terms of a_0^*) monotonically and systematically reaches a plateau value, when those elements not mobilized or involved less in the mechanism are progressively

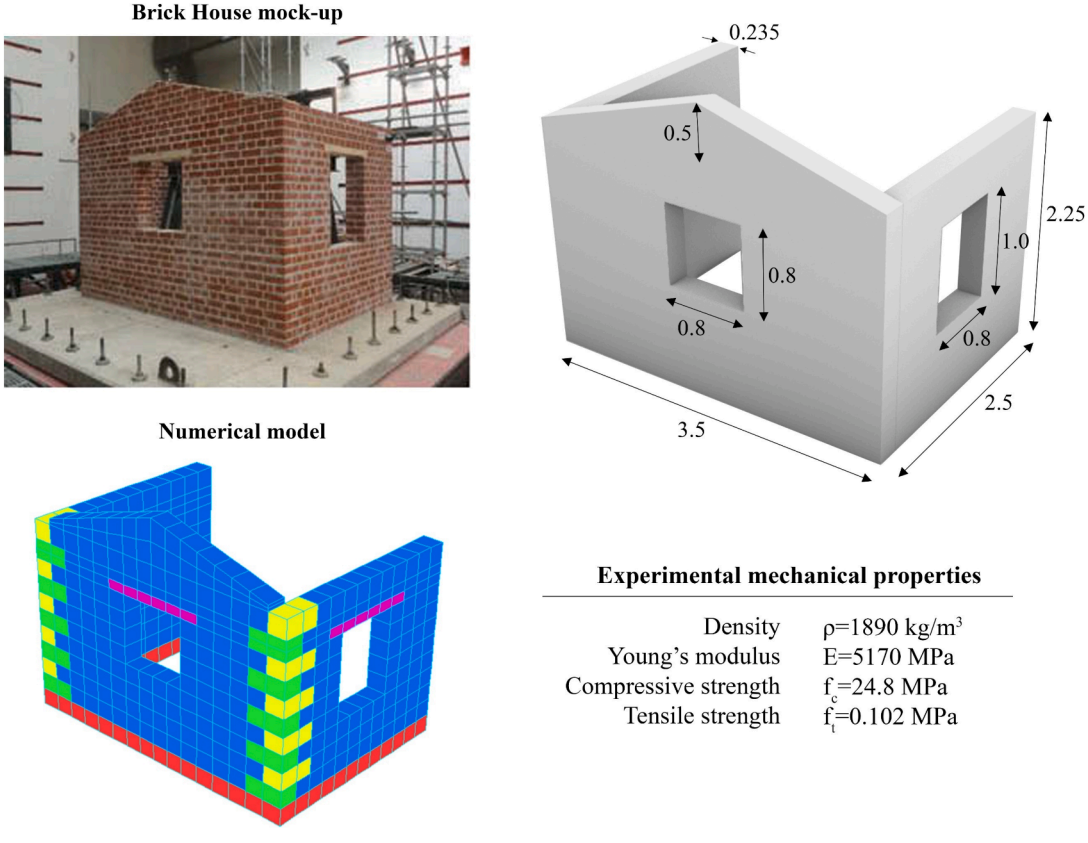

Fig. 2. Geometry and material properties of the brick house tested in [81,82]. All measures are in meters.

excluded through the filter. Accurate evaluations for a_0^* may be obtained assuming heuristically −because no other criterion different from an ex-post rating can be proposed- a threshold for exclusion, which is identified according to a maximum overestimation of the plateau value equal to 20 %. It is also crucial to make a qualitative comparison between the obtained filtered mechanism and the initial one. Adopting such selection criterion, authors experienced −as it will be discussed hereafter when dealing with applications- that the procedure works correctly when elements exhibiting horizontal velocities less than 10–20 % of the maximum one are excluded.

Regarding the final safety assessment, according to [27,28], a masonry structure is considered safe against the activation of a local mechanism if the following inequality is satisfied:

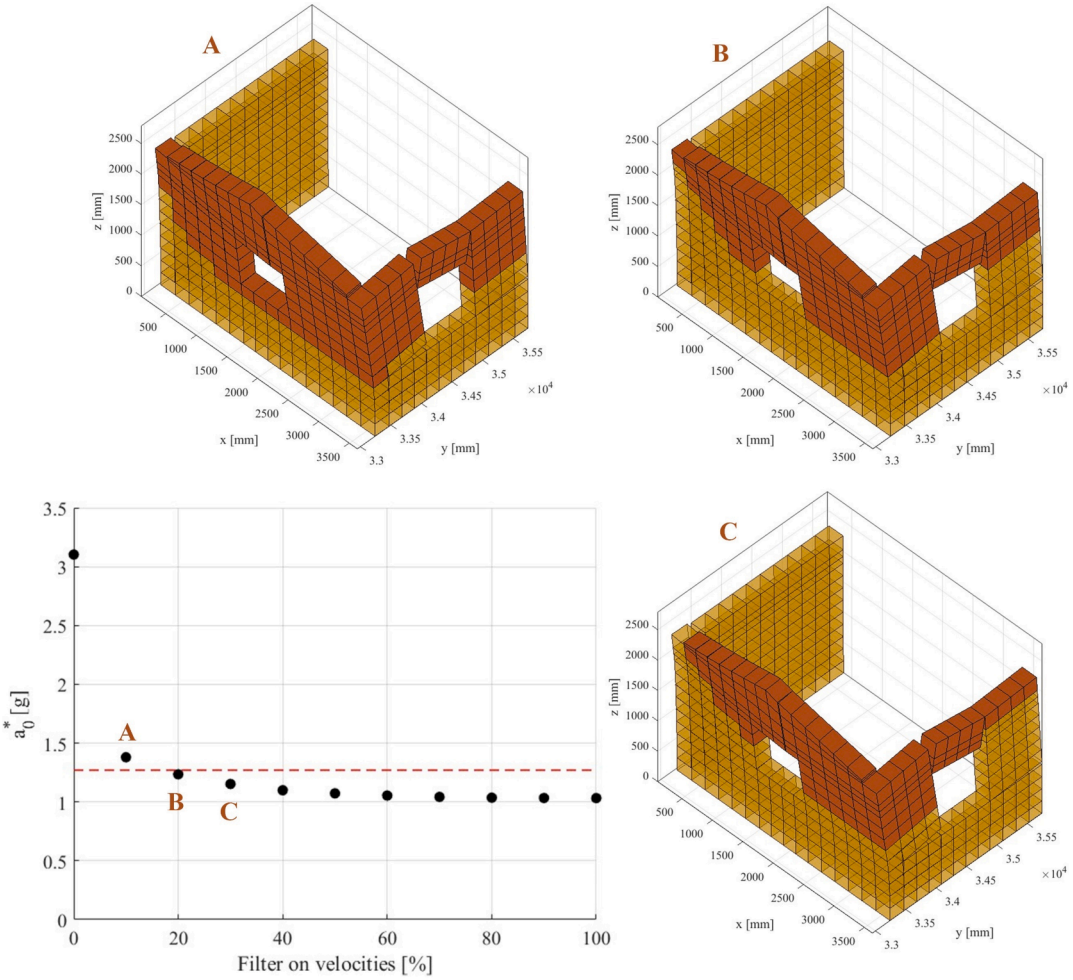

Fig. 3. Comparison between experimental and numerical LA results for the brick house used to benchmark the approach proposed. When a 100% filter is applied, only the elements with maximum horizontal velocity are considered active.

$$a_0^* \geq \frac{a_g S}{q} \tag{18}$$

where a_g is the peak ground acceleration for the site where the structure is located (bedrock assumption), S is a soil and topography coefficient and q is the behaviour factor (generally assumed equal to 2 for masonry structures, as suggested by the building code [28,80]).

It is worth noting that a_0^*, which may be estimated using either pre-assigned failure mechanisms or the novel finite element approach proposed, is evaluated in the paper with the second approach, after the application of the filter. The utilization of a FE approach is belived necessary, as already mentioned, because the assumption of pre-assigned failure mechanisms is responsible for an overestimation of the collapse acceleration in presence of complex crack patterns.

3. Software benchmarking

The method proposed in Section 2 is benchmarked on a "brick house" tested at the LNEC shaking table in Lisbon (Portugal) [81,82]. The specimen was built using perforated clay bricks with an English bond arrangement and cement-based mortar. The mock-up presents a U-shaped plan and three walls: the façade and two sidewalls acting as abutments. The façade has a central window and a gable on the top, instead the sidewalls are one without perforation and the other with a central window, as shown in Fig. 2. The

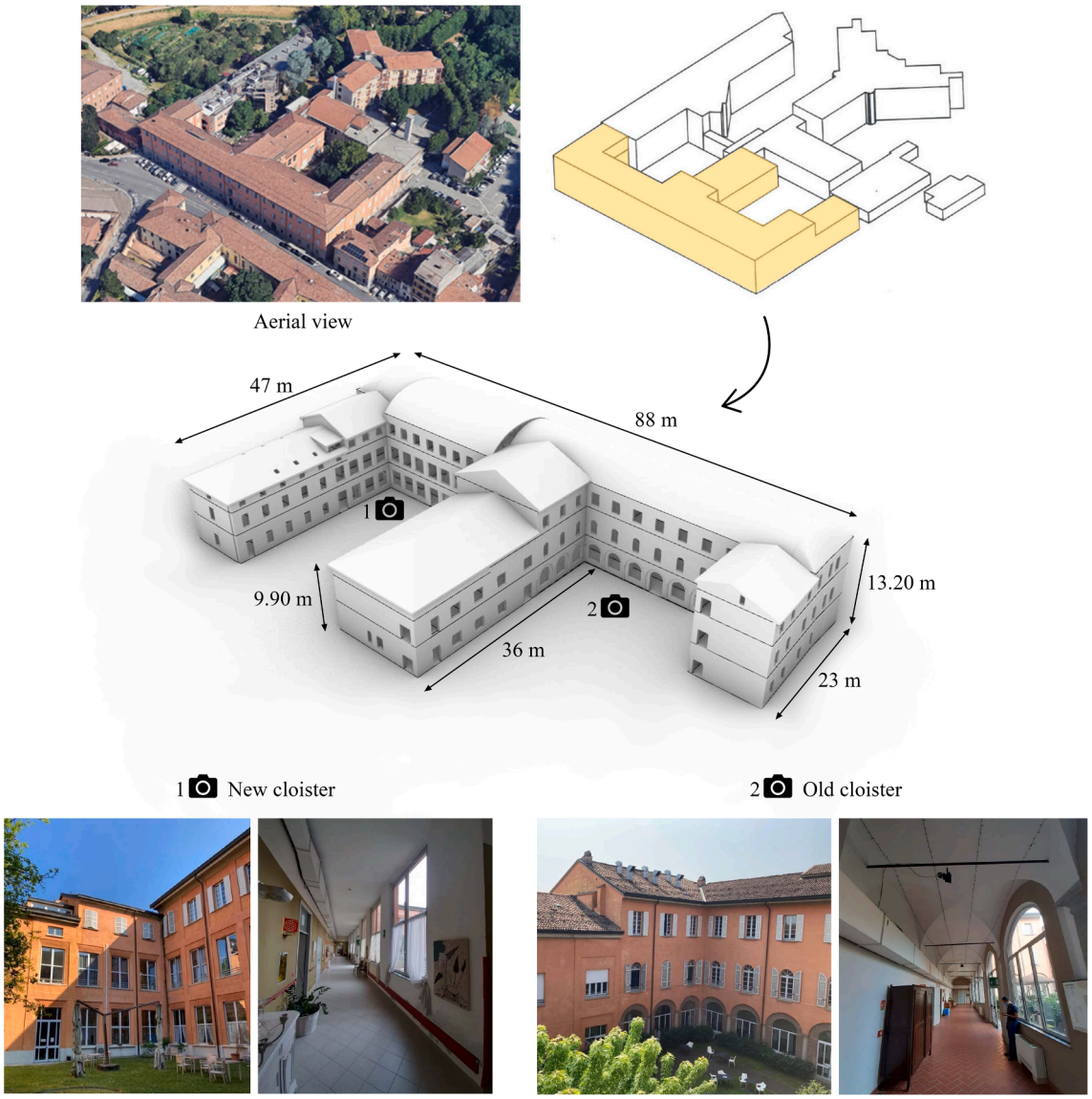

Fig. 4. Case Study 1: Vittorio Emanuele II palace.

structure was subjected to a unidirectional ground motion perpendicular to the façade. Some wallettes made with the same brick masonry were tested under vertical and diagonal compression, to identify the mechanical parameters of the structure, such as the Young's modulus, the tensile and compressive strength, and the density, which are reported in Fig. 2.

The numerical model of the brick house is built according to [81,82], assuming the mechanical parameters identified with the experimental tests −exception made for the elastic modulus-. The structure is studied under a G1 horizontal load distribution perpendicular to the façade. The collapse spectral acceleration is computed according to the procedure described in Section 2, based on the Italian standards and the new filtering algorithm to compute the participating mass. In this case the collapse acceleration a_g/g is evaluated for the experimental value of tensile strength ($f_t = 0.102MPa$), and not for a no-tension material ($f_t = 0$), since the experimental strength is already available.

The results in terms of collapse spectral accelerations a_0^* and collapse mechanisms found with the proposed filtering algorithm −with different filter thresholds- are collected in Fig. 3.

It is worth noting that if all the elements of the structure, even those having very small horizontal velocities, are considered to evaluate the participating mass M^*, the collapse spectral acceleration a_0^* is overestimated. In this case, indeed, a value of $3.10g$ is found, which is much higher than the experimental one, equal to $1.27g$. On the contrary, if a filter on the horizontal velocities is applied to correctly evaluate the participating mass M^*, the values found for the collapse spectral acceleration a_0^* are much more in agreement with the experimental one. Applying a filter that considers only the elements with a horizontal velocity greater than 10%, 20%, and 30% of the maximum one, the values of the collapse acceleration found are respectively equal to $1,38g$, $1,24g$ and $1,15g$, with percentage errors respectively equal to 8.66%, 2.75%, and 9.24% (see points A, B, C of Fig. 3). Moreover, looking at the collapse mechanisms found for points A, B, C of Fig. 3, it is evident the similarity with the experimental one.

According to the results, the proposed filtering algorithm, which considers only the elements having a horizontal velocity greater than 20 % of the maximum one, is effective in identifying both the collapse spectral acceleration and the active mechanism, with an error smaller than 3 %.

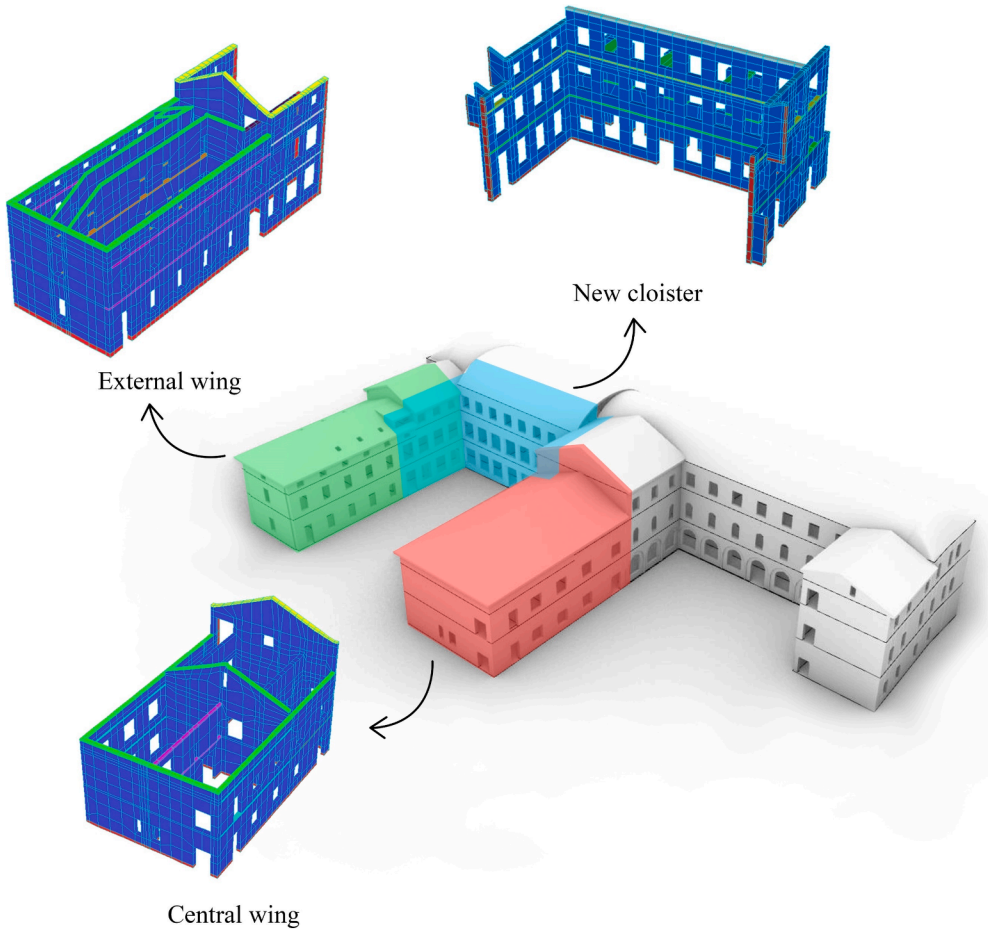

Fig. 5. Analyzed portions of Case Study 1.

4. Practical applications

The seismic vulnerability of two historical masonry structures located in Piacenza, in northern Italy, namely the so-called Vittorio Emanuele II palace (Case Study 1) and the so-called former monastery of Santa Maria della Pace (Case Study 2), is assessed by adopting the numerical approach explained in Section 2. The geometric features of the structures as well as their historical evolution are described in the following subsections.

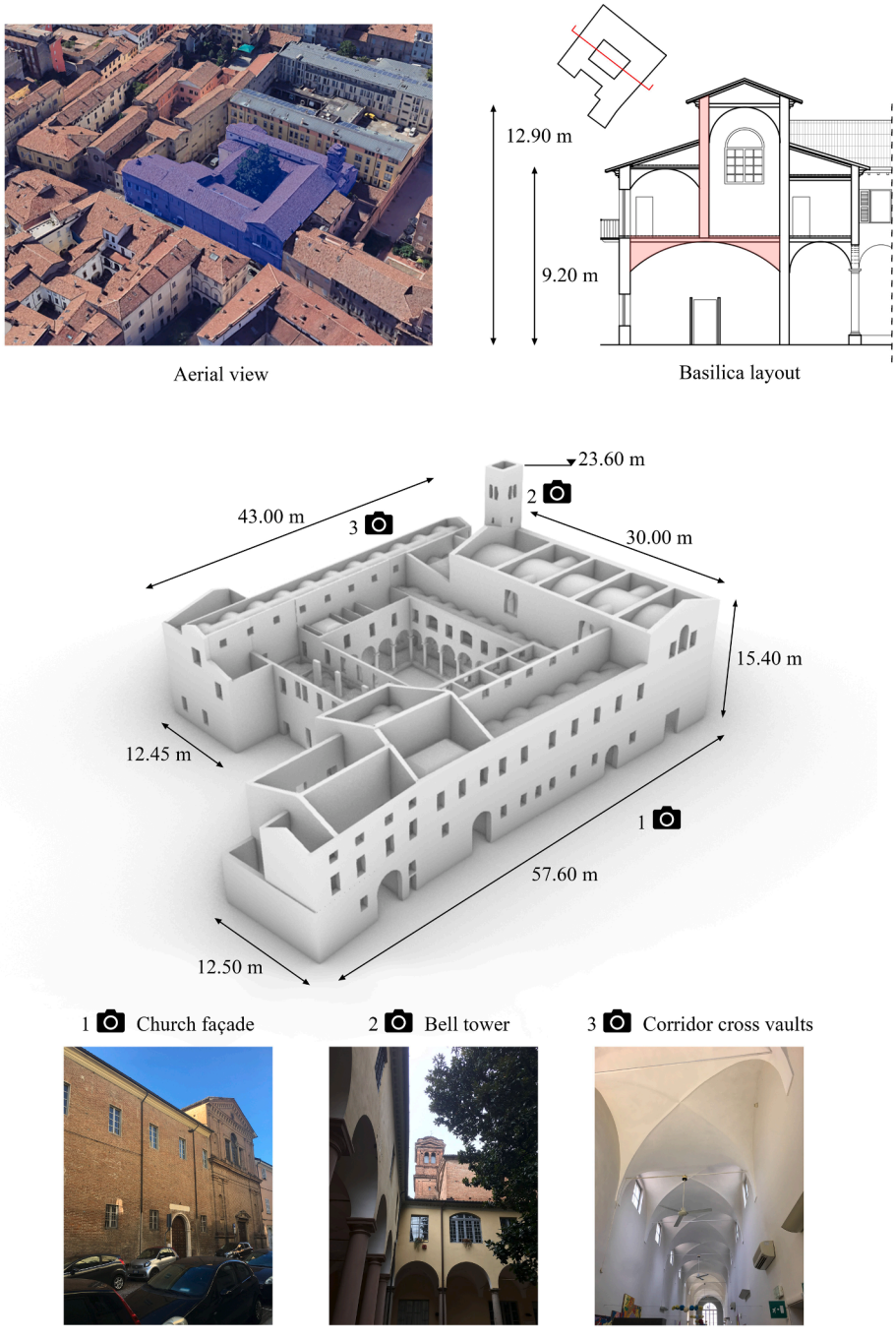

Fig. 6. Case Study 2: former monastery of Santa Maria della Pace.

4.1. Case Study 1 – Critical historical analysis of Vittorio Emanuele II palace

Case Study 1 is an old building complex located in Piacenza, northern Italy, which is the result of many structural changes over time. The oldest portion of the Vittorio Emanuele II palace is characterised by an 'E' shape, highlighted in yellow in Fig. 4. It is constituted by three above-ground floors and a basement. Initially, only a small portion of the building constituted by two floors was present, the so-called Randani-Tedeschi palace which dates to 1670. Then the palace was enlarged in 1882 and the three wings were built in 1912. Finally, in 1956 the whole building was raised to one floor. The three wings create two internal courtyards, named Old Cloister and New Cloister in Fig. 4 according to the age of construction. The old portion of the building features many cloisters and cross vaults, and it corresponds to the previous Randani-Tedeschi palace. Traces of the latter are visible in the Old Cloister characterised by the presence of many cross vaults (see Fig. 4).

The possible activation of local collapse mechanisms is evaluated by analysing large portions of the structure, which are those highlighted in Fig. 5, which also shows the structural models. The portions analysed correspond to the biggest wings of the structure, namely the External and Central wings, and the New Cloister. These portions belong to the most recent part of the structure built in the 1950 s. It features thin walls and few orthogonal walls giving a bracing action; therefore, it is the most vulnerable part of the structure against horizontal seismic actions. In all structural models, the floors and the roof are not directly modelled due to their poor connection with walls. Conversely, their presence is taken into account as far as the vertical load application is concerned, which is considered adding distributed masses at storey levels, and depicted in Fig. 5 using different colours for the hexahedron elements. The precise amount of such masses is evaluated considering the self-weigh of the roof and floors, their static scheme, and the corresponding influence area as far as dead and live loads are concerned.

4.2. Case study 2 – Critical historical analysis of the former monastery of Santa Maria della pace

The former monastery of Santa Maria della Pace, located in Piacenza (northern Italy), was built by the commission of the Benedictine nuns in the 16th century. The portion of the structure that is still standing nowadays was not subjected to meaningful structural changes [35,83]. The former monastery features a two-level cloister layout, as shown in Fig. 6. Cross vaults characterize the cloisters and the corridors of the first floor, while the rooms are mainly covered by cloister vaults and sometimes by timber floors. The timber roof covering the structure is pitched and it is characterized by different heights according to the geometry in elevation of the structure.

The portions of the structure analysed by means of the numerical approach proposed in Section 2 are shown in Fig. 7. They represent the most vulnerable parts of the building. Indeed, the church is characterised by long longitudinal walls and the presence of a bell tower partially embedded into one of the rear corners. The architecture of the wing with a basilica layout on the ground floor is characterized by the presence of a big room (originally used as a refectory) covered by a cloister vault, which bears at the keystone one

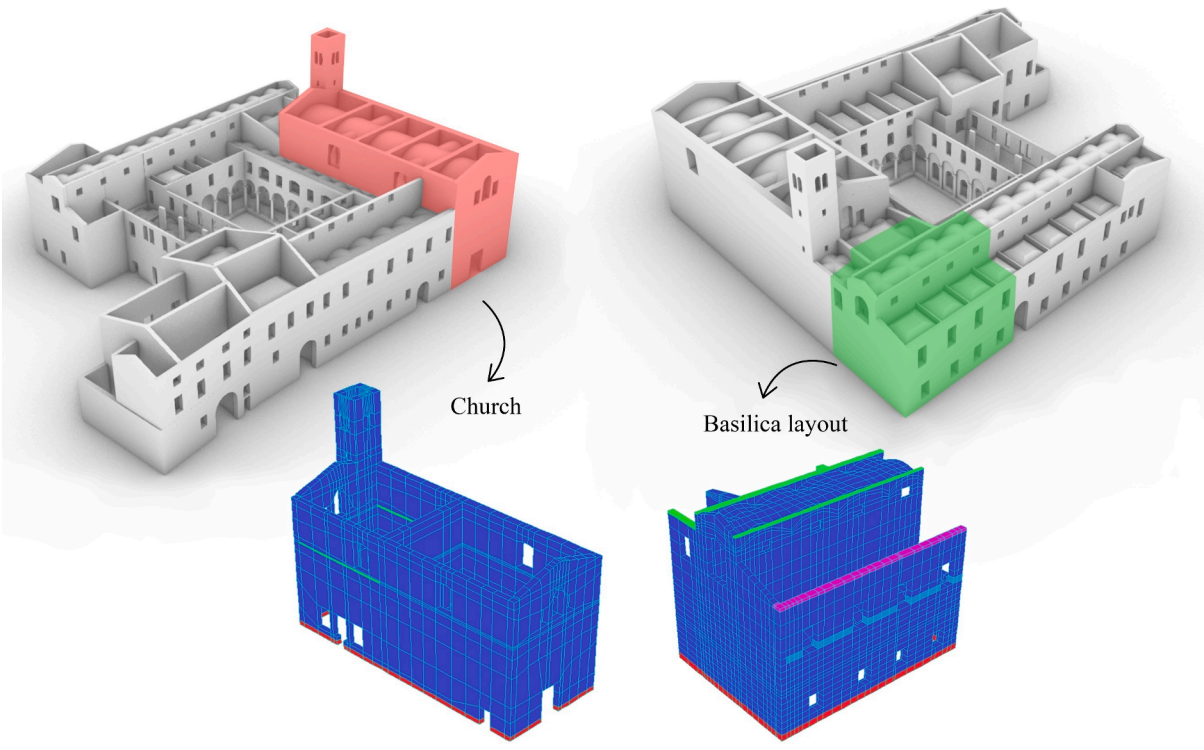

Fig. 7. Analysed portions of Case Study 2.

of the two longitudinal external walls of the first floor [83], see the Basilica Layout section depicted in Fig. 6 where the longitudinal wall of the first floor and the vault at the ground floor are coloured in red.

The structural models shown in Fig. 7 include the presence of timber roofs and floors through the application of distributed masses,

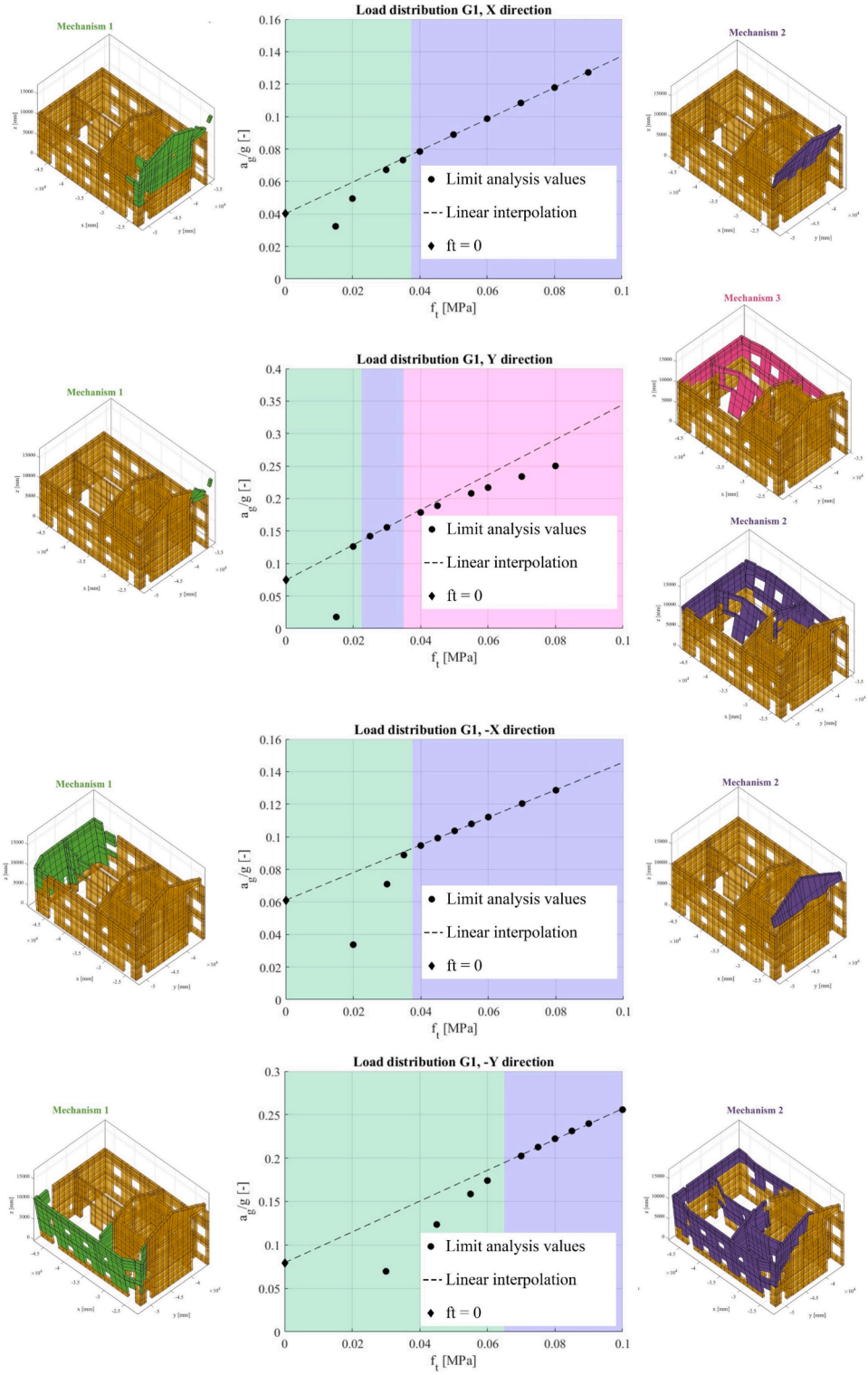

Fig. 8. Collapse acceleration vs tensile strength and active failure mechanisms of the Central Wing under G1 load distribution.

as done for Case Study 1.

5. Results and discussion

In this section, the spectral accelerations a_0^* that trigger local failure mechanisms are evaluated considering two load distributions, namely G1 and G2, and different entrance angles of the seismic load. The structural performance is verified against the design seismic action for a specific limit state. The seismic capacity of the portions belonging to Case Study 1 and Case Study 2 is compared with the seismic hazard prescribed by the Italian building code, referring to the construction site. The selected design seismic action corresponds to the life safety limit state with a return period T_R of 457 years, characterised by a bedrock acceleration equal to $a_g = 0.092g$. Furthermore, according to the stratigraphy [84] and in agreement with Italian standards [27], the soil type of the construction site and the topography class are classified as C and T1 respectively, leading to a soil and topography coefficient S equal to 1.5. Hence, according to Eq. (18), the local failure mechanism is not triggered if:

$$a_0^* \geq \frac{a_g S}{q} = 0.677 m/s^2 \tag{19}$$

5.1. Case Study 1 – Limit analysis results for Vittorio Emanuele II palace

As discussed in Section 4, only some portions of the Vittorio Emanuele II palace are analysed, namely the Central Wing, the External Wing, and the New Cloister. As far as the Central Wing is concerned, the results obtained are summarized in Fig. 8. They are represented in terms of collapse accelerations a_g/g at progressively reduced tensile strength, assuming the seismic load angle entrance is oriented along the two main geometric directions of the structure, both positive and negative, under a load distribution G1. Through a linear extrapolation of the results in each direction, the collapse acceleration a_g/g for a no-tension material $(f_t = 0MPa)$ is derived. Collapse accelerations associated with failure mechanisms affected by spurious sliding of the blocks are disregarded when performing the linear extrapolation.

Starting from the collapse acceleration a_g/g obtained for the no-tension material assumption, the collapse spectral acceleration that triggers the local failure mechanism is computed and compared with the design acceleration, which is defined as $a_g S/q$ for the site where the structure is located (as explained in Section 5 for the definition of Eq. (19)). The results obtained are summarized in Fig. 9, both in terms of spectral acceleration and active local failure mechanism in the four loading directions. As it is possible to notice, the structure is verified only along the Y-negative direction. Considering the results found in Section 3 for the benchmark structure, also in the present applications, the collapse spectral acceleration is computed considering only elements having a horizontal velocity greater than 20 % of the maximum one, as shown in Fig. 9. Indeed, from the sensitivity analysis shown in Fig. 10 for the Central Wing under a G1 horizontal load distribution applied along the Y-negative direction, it is evident that the trend of the collapse spectral acceleration in function of the filter on the velocities is the same found for the benchmark structure. Also in this case, looking at Fig. 10, it appears evident that, if the elements with very small velocities are considered in the calculation of the participating mass, the collapse spectral

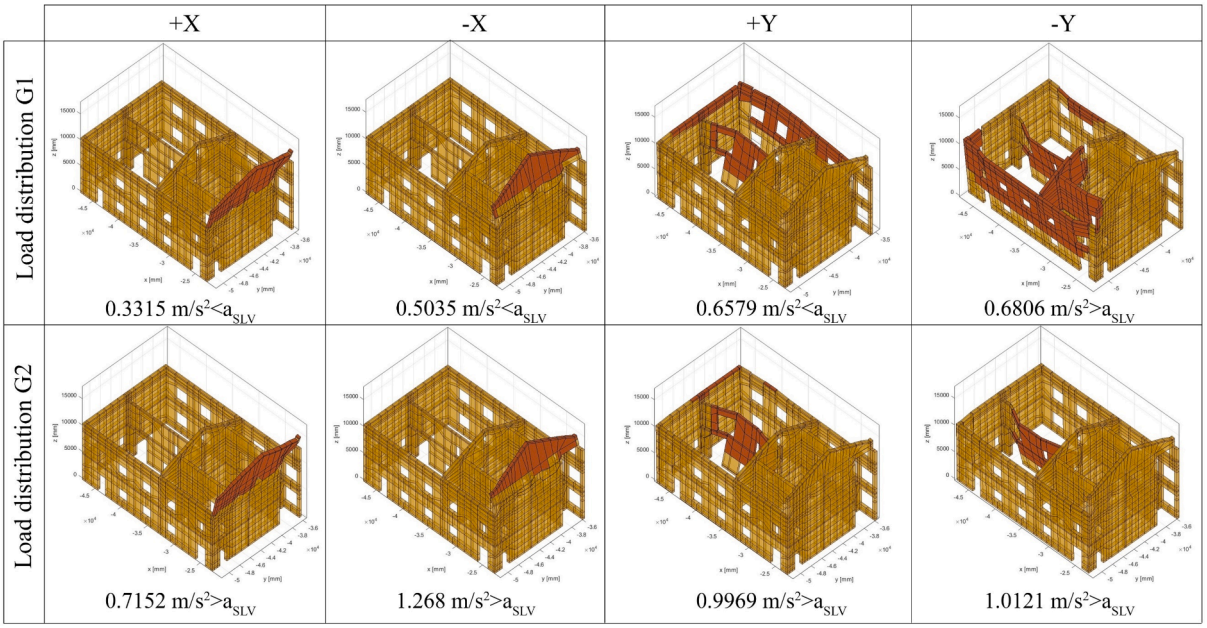

Fig. 9. Spectral accelerations triggering local failure mechanisms for the Central Wing under G1and G2 load distributions.

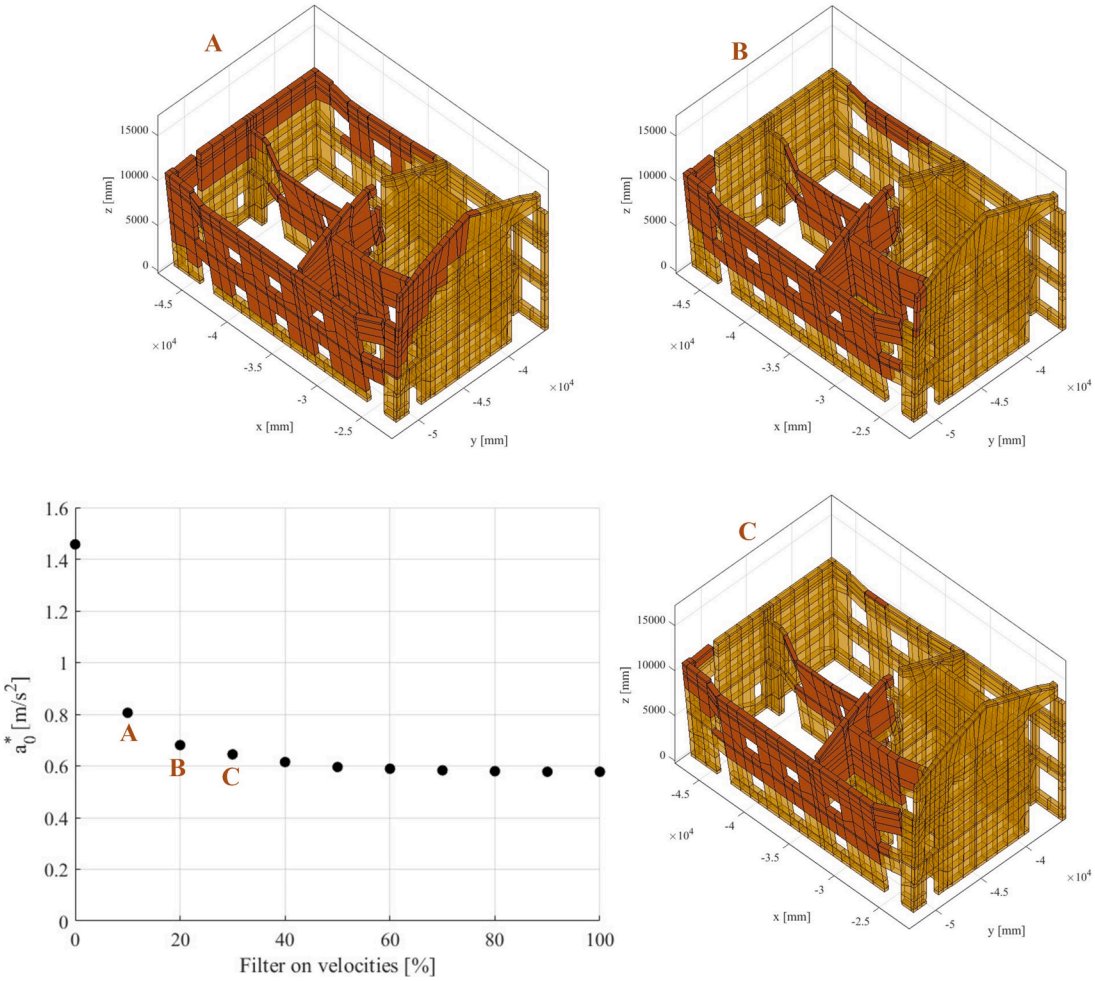

Fig. 10. Sensitivity analysis of the filtering algorithm for the Central Wing under G1 load distribution along Y-negative direction. When a 100% filter is applied only the elements with maximum horizontal velocity are considered active.

acceleration is overestimated. The same procedure is followed for the Central Wing under G2 load distribution. The collapse acceleration a_g/g for the no-tension material assumption is reported in Fig. 11. Then, the collapse spectral acceleration is computed for each loading direction, as depicted in Fig. 9. For the G2 load distribution, the structure is verified both along positive and negative X and Y directions. Comparing the results obtained for G1 and G2 (Fig. 9) distributions, it is evident that the worst loading condition is that corresponding to the G1 distribution. The structure is not verified, meaning that strengthening interventions are needed.

The same methodology is applied to the External Wing and the New Cloister. For the sake of brevity, results are shown only in terms of a_g/g vs f_t, for G1 and G2 load distributions, while active failure mechanisms and collapse spectral accelerations are shown only applying a filter on the velocities equal to 20 %, which is an assumption on the safe side.

For what concerns the External Wing, the linear extrapolations to find a_g/g for $f_t = 0MPa$ under G1 and G2 load distributions (both X and Y directions) are shown in Fig. 12. It is worth noting that, in the evaluation of the collapse acceleration for a no-tension material in the X-negative direction, and represented in yellow in Fig. 12, under both G1 and G2 loading conditions, the value of the collapse acceleration associated with a tensile strength equal to $0.03MPa$ has been neglected since affected by a sudden decrease of the load carrying capacity and associated to spurious sliding. In Fig. 13, the computed collapse spectral accelerations for the two load distributions with the corresponding active local mechanisms are shown. The structure is verified only in the X-positive direction for both loading conditions. G1 represents the worst horizontal load distribution for this portion of the structure, except for the X-negative direction, where two different collapse mechanisms are triggered. Specifically, G1 activates only the overturning of the tympanum, while G2 is involved in the mechanism of the entire façade and a portion of the perpendicular walls.

The last portion of Vittorio Emanuele II palace analysed is the New Cloister. In this case, only the out-of-plane behaviour of the longest wall is studied. Fig. 14 depicts the linear extrapolation carried out to find the a_g/g for $f_t = 0MPa$ under G1 and G2 load distributions, with the seismic load applied in the direction perpendicular to the longest wall of the cloister. It is evident that the collapse acceleration associated with an $f_t = 0.03MPa$ in the X positive direction is very small. It is also associated with a non-negligible spurious sliding of some of the elements and hence disregarded in the computations. The results in terms of collapse spectral

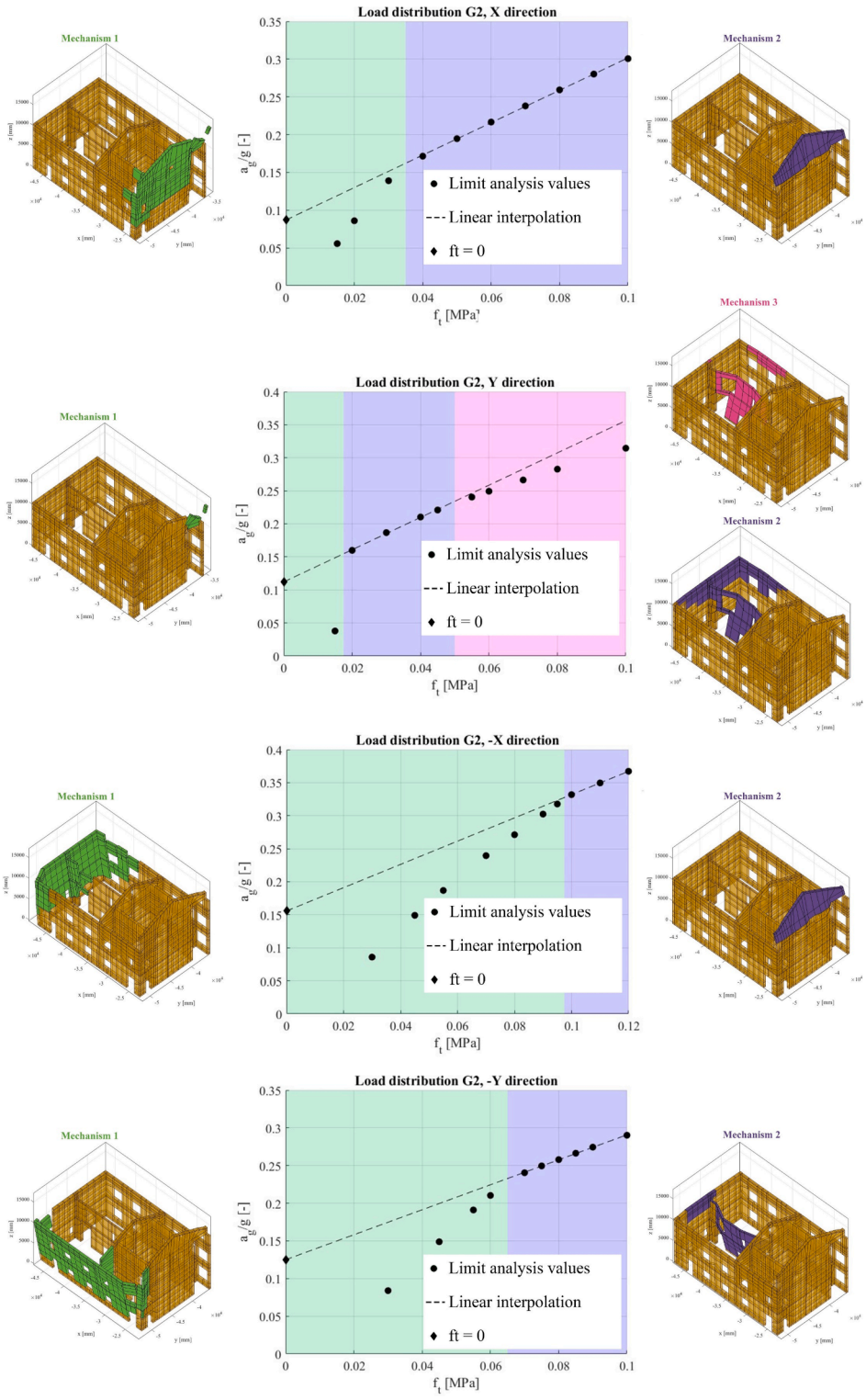

Fig. 11. Collapse acceleration vs tensile strength and active failure mechanisms of the Central Wing under G2 load distribution.

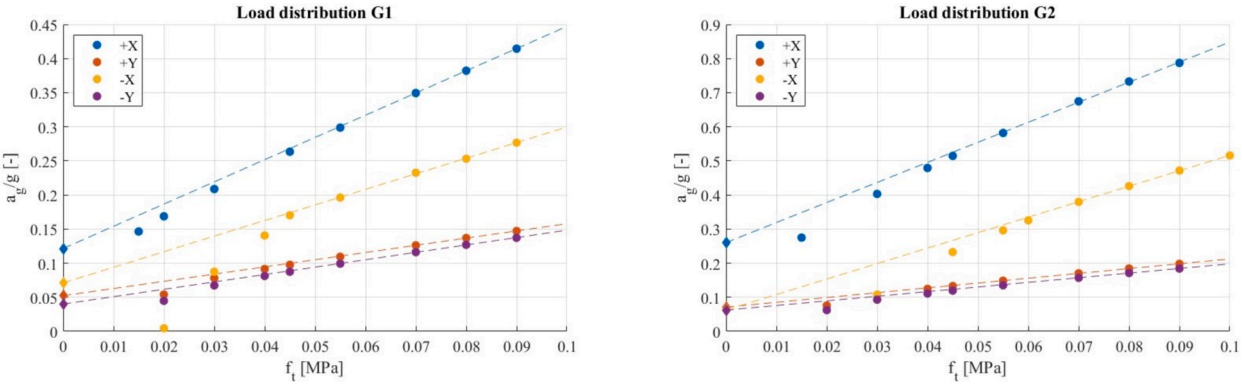

Fig. 12. Collapse acceleration vs tensile strength of the External Wing under G1 and G2 load distributions.

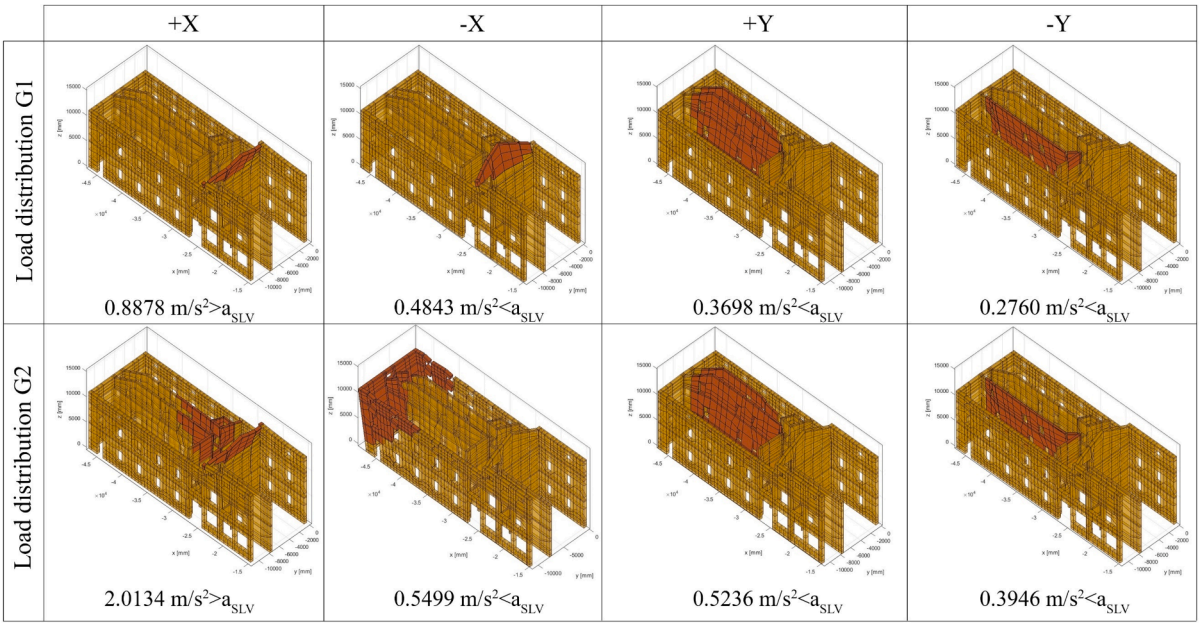

Fig. 13. Spectral accelerations triggering local failure mechanisms of the External Wing under G1 and G2 load distributions.

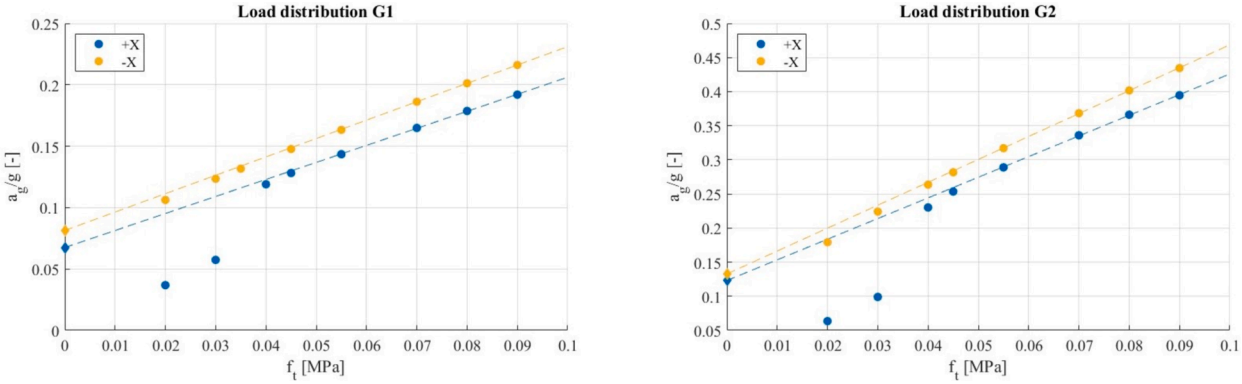

Fig. 14. Collapse acceleration vs tensile strength of the New Cloister under G1 and G2 load distributions.

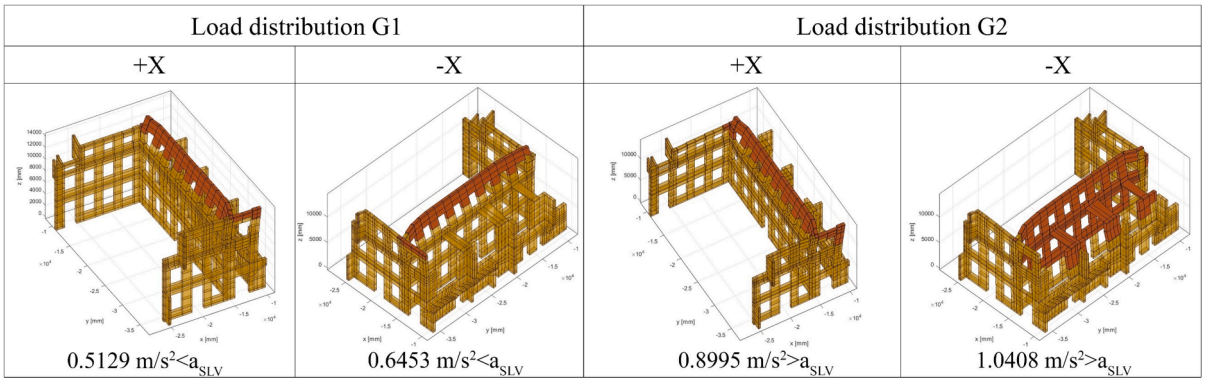

Fig. 15. Spectral accelerations triggering local failure mechanisms of the New Cloister under G1 and G2 load distributions.

accelerations and active local mechanisms are summarized in Fig. 15. The structure is verified only for the G2 distribution.

5.2. Case study 2 – Limit analysis results for the former monastery of Santa Maria della pace

In this section, limit analysis results for the most vulnerable portions of the former monastery of Santa Maria della Pace are shown. Particular attention is devoted to analyzing the Church and the wing with Basilica Layout, as discussed in Section 4. The same procedure already described in detail for the Central Wing of Vittorio Emanuele II palace is followed. For the sake of brevity, results are shown only in terms of a_g/g vs f_t for G1 and G2 load distributions. Furthermore, as far as failure mechanisms active and collapse spectral accelerations are concerned, only the results obtained assuming a filter with a threshold on velocities equal to 20 % are reported.

Fig. 16 and Fig. 17 show, for the Church, respectively the linear extrapolations carried out to obtain the no-tension solution and the active failure mechanisms, along with the associated collapse spectral accelerations. From the results, it can be deduced that the most vulnerable parts are the bell tower and the longitudinal walls of the single nave. The structure is verified, considering the actual design seismic action at the ultimate limit state, only along the X-positive and Y-negative directions, when a uniform distribution of horizontal loads along the height (G2) is applied.

When dealing with the Basilica wing, the structure is analyzed only considering horizontal forces perpendicular to the longitudinal walls, being the most vulnerable when loaded out-of-plane. According to the results obtained, shown in Fig. 18 (obtainment of the no-tension material collapse accelerations) and Fig. 19 (collapse mechanisms), the structure is characterized by a collapse spectral acceleration lower than the design seismic one for G1 load distribution, while is verified under the G2 load distribution.

Since both portions of the former monastery analysed are not verified according to Italian standards, strengthening interventions are needed.

6. Conclusions

In this work, a novel Finite Element upper-bound limit analysis equipped with a novel velocity filtering routine has been proposed to assess masonry structures with complex geometry against the activation of local collapse mechanisms. The methodology has been conceived to be completely in agreement with Italian standard requirements, at the same time having the advantage that the definition of pre-assigned failure mechanisms is not required. The method has involved discretizing the structure into infinitely resistant hexahedron elements, with plastic deformation occurring only at the interfaces between adjoining elements. This assumption has led to formulating a classic linear programming problem into few independent variables, which are represented by the generalized velocities of the hexahedron elements and the plastic multipliers of the quadrilateral interfaces. Having discretized the domain with infinitely resistant elements with plasticity concentrated on a finite number of interfaces, to detect rigorously the crack pattern at failure is not possible, but (i) the upper bound has coincided with the lower bound, allowing in principle to obtain the static solution via solving a self-dual linear programming problem and (ii) the computational burden has dropped down, thus allowing the analysis of complex case-studies. In the spirit of the Upper Bound theorem, the results have been expressed in terms of collapse acceleration and active failure mechanisms. As Italian standards prescribe the adoption for masonry of a vanishing tensile strength without sliding, the collapse acceleration – calculated as the base shear divided by vertical loads – has been indirectly determined through linear extrapolation, a stratagem to avoid both undesired premature halting or stalling of the numerical algorithm and the activation of parasite sliding between adjacent elements.

This methodology has offered several advantages. The analyses have been fast, and the MATLAB code developed by the authors only required the mesh definition and the parameters for the Mohr-Coulomb strength criterion definition. Additionally, the spectral acceleration that has triggered local failure has been identified without pre-selecting specific failure mechanisms, enabling an automatized analysis of complex geometries, where predicting the failure mechanism shape in advance is challenging.

The final innovation presented relied upon the implementation of a filtering strategy to select only the elements contributing in a

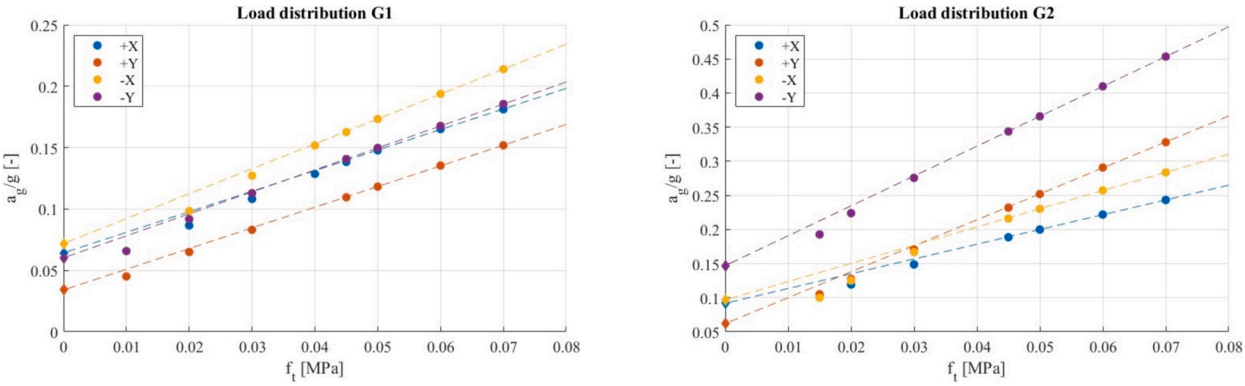

Fig. 16. Collapse acceleration vs tensile strength of the Church under G1 and G2 load distributions.

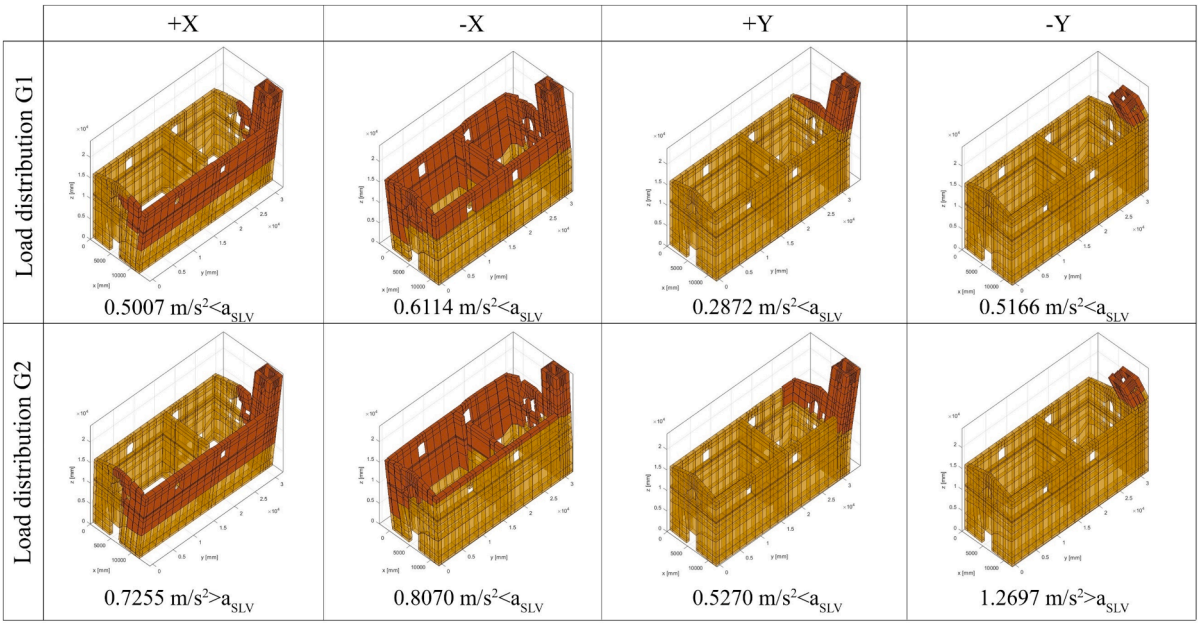

Fig. 17. Spectral accelerations triggering local failure mechanisms of the Church under G1 and G2 load distributions.

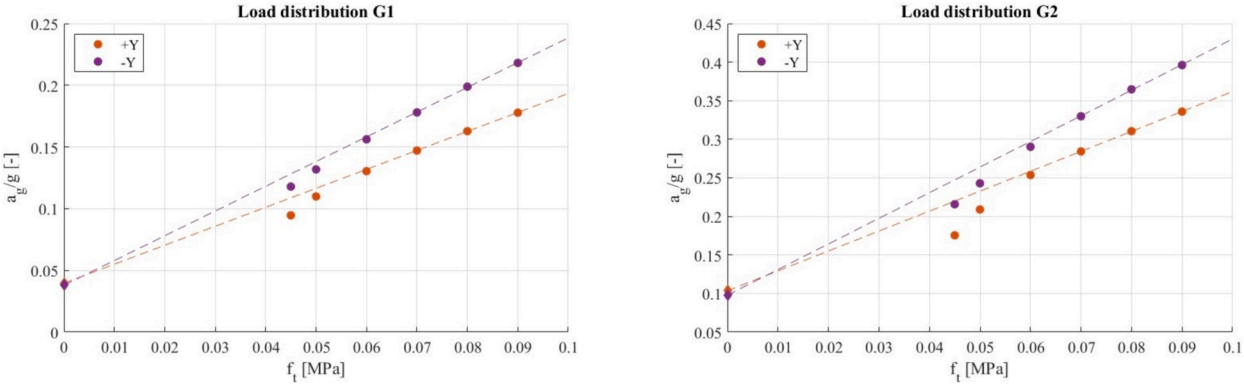

Fig. 18. Collapse acceleration vs tensile strength of the Basilica Layout under G1 and G2 load distributions.

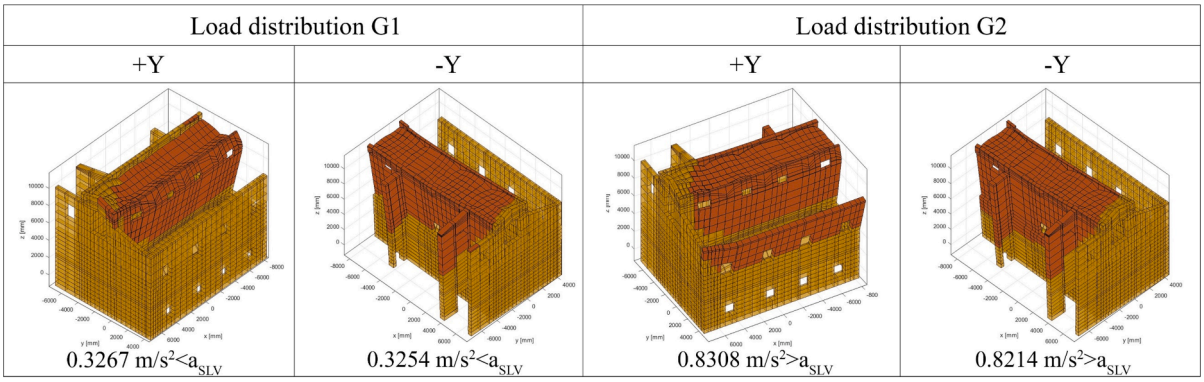

Fig. 19. Spectral accelerations triggering local failure mechanisms of the Basilica Layout under G1 and G2 load distributions.

significant way to the activation of the mechanism, a feature that allowed the determination of the collapse spectral acceleration to be used in verifications at the ultimate limit state carried out according to Italian national norms.

The procedure has been validated on two case studies located in Piacenza, northern Italy, namely the Vittorio Emanuele II palace and the former monastery of Santa Maria della Pace. Both case studies exhibit a high level of complexity, making it almost impossible to obtain a reliable prediction of the failure accelerations using standard procedures available. The analyses have been conducted on the significant portions of the structures, characterized by peculiar geometries. The results have revealed that strengthening interventions are necessary on both structures, as the design seismic action defined by the building code for the site of Piacenza could trigger some local collapses.

CRediT authorship contribution statement

Martina Buzzetti: Writing – review & editing, Writing – original draft, Validation, Methodology, Investigation, Data curation, Conceptualization. **Natalia Pingaro:** Writing – review & editing, Writing – original draft, Validation, Methodology, Investigation, Data curation, Conceptualization. **Gabriele Milani:** Writing – review & editing, Writing – original draft, Supervision, Methodology, Investigation, Data curation, Conceptualization.

Declaration of competing interest

The authors declare that they have no known competing financial interests or personal relationships that could have appeared to influence the work reported in this paper.

Data availability

Data will be made available on request.

References

[1] A. Shabani, M. Kioumarsi, M. Zucconi, State of the art of simplified analytical methods for seismic vulnerability assessment of unreinforced masonry buildings, Eng Struct 239 (2021) 112280, https://doi.org/10.1016/j.engstruct.2021.112280.
[2] L. Sorrentino, D. D'Ayala, G. de Felice, M.C. Griffith, S. Lagomarsino, G. Magenes, Review of out-of-plane seismic assessment techniques applied to existing masonry buildings, International Journal of Archit. Herit. 11 (2017) 2–21, https://doi.org/10.1080/15583058.2016.1237586.
[3] L. Decanini, A. De Sortis, A. Goretti, R. Langenbach, F. Mollaioli, A. Rasulo, Performance of masonry buildings during the 2002 Molise, Italy, earthquake, Earthq. Spectra 20 (2004) (2002) S191–S220, https://doi.org/10.1193/1.1765106.
[4] D.F. D'Ayala, S. Paganoni, Assessment and analysis of damage in L'Aquila historic city centre after 6th April 2009, Bull. Earthq. Eng. 9 (2011) 81–104, https://doi.org/10.1007/s10518-010-9224-4.
[5] A. Penna, P. Morandi, M. Rota, C.F. Manzini, F. da Porto, G. Magenes, Performance of masonry buildings during the Emilia 2012 earthquake, Bull. Earthq. Eng. 12 (2014) 2255–2273, https://doi.org/10.1007/s10518-013-9496-6.
[6] L. Sorrentino, S. Cattari, F. da Porto, G. Magenes, A. Penna, Seismic behaviour of ordinary masonry buildings during the 2016 central Italy earthquakes, Bull. Earthq. Eng. 17 (2019) (2016) 5583–5607, https://doi.org/10.1007/s10518-018-0370-4.
[7] G. Vlachakis, E. Vlachaki, P.B. Lourenço, Learning from failure: Damage and failure of masonry structures, after the 2017 Lesvos earthquake (Greece), Eng Fail Anal 117 (2020) 104803, https://doi.org/10.1016/j.engfailanal.2020.104803.
[8] M. Acito, M. Buzzetti, C. Chesi, E. Magrinelli, G. Milani, Failures and damages of historical masonry structures induced by 2012 northern and 2016–17 central Italy seismic sequences: Critical issues and new perspectives towards seismic prevention, Eng Fail Anal 149 (2023) 107257, https://doi.org/10.1016/j.engfailanal.2023.107257.
[9] E. Işık, F. Avcil, A. Büyüksaraç, R. İzol, M. Hakan Arslan, C. Aksoylu, E. Harirchian, O. Eyisüren, E. Arkan, M. Şakir Güngür, M. Günay, H. Ulutaş, Structural damages in masonry buildings in Adıyaman during the Kahramanmaraş (Turkiye) earthquakes (Mw 7.7 and Mw 7.6) on 06 February 2023, Eng Fail Anal 151 (2023) 107405. Doi: 10.1016/j.engfailanal.2023.107405.
[10] J.B. Rondelet, Traite Theorique Et Pratique De L'art De Batir., Paris, 1812.
[11] J. Heyman, The stone skeleton, Int J Solids Struct 2 (1966), https://doi.org/10.1016/0020-7683(66)90018-7.

[12] F. Portioli, C. Casapulla, M. Gilbert, L. Cascini, Limit analysis of 3D masonry block structures with non-associative frictional joints using cone programming, Comput Struct 143 (2014) 108–121, https://doi.org/10.1016/j.compstruc.2014.07.010.
[13] L. Cascini, G. Brando, F.P.A. Portioli, M.R. Forgione, C. Mazzanti, M. Vasta, Force-based seismic evaluation of retrofitting interventions of historic masonry castles by 3D rigid block limit analysis, Applied Sciences (Switzerland) 10 (2020) 5035, https://doi.org/10.3390/app10155035.
[14] M.F. Funari, A. Mehrotra, P.B. Lourenço, A tool for the rapid seismic assessment of historic masonry structures based on limit analysis optimisation and rocking dynamics, Applied Sciences (Switzerland) 11 (2021) 1–22, https://doi.org/10.3390/app11030942.
[15] A. Iannuzzo, A. Dell'Endice, T. Van Mele, P. Block, Numerical limit analysis-based modelling of masonry structures subjected to large displacements, Comput Struct 242 (2021) 106372, https://doi.org/10.1016/j.compstruc.2020.106372.
[16] C. Casapulla, A. Maione, F. Ceroni, A. Prota, M. Di Ludovico, Limit analysis and design-oriented approach for out-of-plane loaded masonry walls strengthened by grouted anchors, Eng Struct 285 (2023) 115991, https://doi.org/10.1016/j.engstruct.2023.115991.
[17] S. Galassi, An alternative approach for limit analysis of masonry arches on moving supports in finite small displacements, Eng Fail Anal 145 (2023) 107004, https://doi.org/10.1016/j.engfailanal.2022.107004.
[18] A. Chiozzi, N. Grillanda, G. Milani, A. Tralli, UB-ALMANAC: An adaptive limit analysis NURBS-based program for the automatic assessment of partial failure mechanisms in masonry churches, Eng Fail Anal 85 (2018) 201–220, https://doi.org/10.1016/j.engfailanal.2017.11.013.
[19] A. Lo Monaco, N. Grillanda, I. Onescu, M. Fofiu, F. Clementi, M. D'Amato, A. Formisano, G. Milani, M. Mosoarca, Seismic assessment of Romanian Orthodox masonry churches in the Banat area through a multi-level analysis framework, Eng Fail Anal 153 (2023) 107539. Doi: 10.1016/j.engfailanal.2023.107539.
[20] A. Cecchi, G. Milani, A kinematic FE limit analysis model for thick English bond masonry walls, Int J Solids Struct 45 (2008) 1302–1331, https://doi.org/10.1016/j.ijsolstr.2007.09.019.
[21] G. Milani, Simple lower bound limit analysis homogenization model for in- and out-of-plane loaded masonry walls, Constr Build Mater 25 (2011) 4426–4443, https://doi.org/10.1016/j.conbuildmat.2011.01.012.
[22] A. Chiozzi, M. Malagù, A. Tralli, A. Cazzani, ArchNURBS: NURBS-based tool for the structural safety assessment of masonry arches in MATLAB, J. Comput. Civ. Eng. 30 (2016) 04015010, https://doi.org/10.1061/(asce)cp.1943-5487.0000481.
[23] B. Nela, A.J. Rios, M. Pingaro, E. Reccia, P. Trovalusci, Masonry arches simulations using cohesion parameter as code enrichment for limit analysis approach, International Journal of Masonry Research and Innovation 9 (2023) 80–95, https://doi.org/10.1504/IJMRI.2024.135236.
[24] G. Milani, Lesson learned after the Emilia-Romagna, Italy, 20–29 May 2012 earthquakes: A limit analysis insight on three masonry churches, Eng Fail Anal 34 (2013) (2012) 761–778, https://doi.org/10.1016/j.engfailanal.2013.01.001.
[25] D. Aita, M. Bruggi, E. Garavaglia, Collapse analysis of masonry arches and domes considering finite friction and uncertainties in compressive strength, Eng Fail Anal 163 (2024) 108462, https://doi.org/10.1016/j.engfailanal.2024.108462.
[26] P. Wang, G. Milani, Specialized 3D Distinct element limit analysis approach for a fast seismic vulnerability evaluation of massive masonry structures: Application on traditional pagodas, Eng Struct 282 (2023) 115792, https://doi.org/10.1016/j.engstruct.2023.115792.
[27] Ministero delle Infrastrutture e dei Trasporti, Decreto 17 gennaio 2018 - Aggiornamento delle "Norme tecniche per le costruzioni," Gazzetta Ufficiale Della Repubblica Italiana (2018).
[28] Ministero delle Infrastrutture e dei Trasporti, Circolare 21 gennaio 2019 n.7: Istruzioni per l'applicazione dell'«Aggiornamento delle "Norme Tecniche per le Costruzioni"» di cui al decreto ministeriale 17 gennaio 2018., Gazzetta Ufficiale Della Repubblica Italiana (2019).
[29] M.J.N. Priestley, SEISMIC BEHAVIOUR OF UNREINFORCED MASONRY WALLS, Bulletin of the New Zealand National Society for Earthquake Engineering 18 (1985) 191–205, https://doi.org/10.5459/bnzsee.18.2.191-205.
[30] K. Doherty, M.C. Griffith, N. Lam, J. Wilson, Displacement-based seismic analysis for out-of-plane bending of unreinforced masonry walls, Earthq Eng Struct Dyn 31 (2002) 833–850, https://doi.org/10.1002/eqe.126.
[31] H. Derakhshan, M.C. Griffith, J.M. Ingham, Out-of-plane behavior of one-way spanning unreinforced masonry walls, J Eng Mech 139 (2013) 409–417, https://doi.org/10.1061/(asce)em.1943-7889.0000347.
[32] H. Derakhshan, D.Y. Dizhur, M.C. Griffith, J.M. Ingham, Seismic assessment of out-of-plane loaded unreinforced masonry walls in multi-storey buildings, Bull. N. Z. Soc. Earthq. Eng. 47 (2014) 119–138, https://doi.org/10.5459/bnzsee.47.2.119-138.
[33] D.F. D'ayala, Force and displacement based vulnerability assessment for traditional buildings, Bull. Earthq. Eng. 3 (2005) 235–265, https://doi.org/10.1007/s10518-005-1239-x.
[34] T.M. Ferreira, A.A. Costa, R. Vicente, H. Varum, A simplified four-branch model for the analytical study of the out-of-plane performance of regular stone URM walls, Eng Struct 83 (2015) 140–153, https://doi.org/10.1016/j.engstruct.2014.10.048.
[35] M. Acito, M. Buzzetti, G.A. Cundari, G. Milani, General methodological approach for the seismic assessment of masonry aggregates, Structures 57 (2023) 105177, https://doi.org/10.1016/j.istruc.2023.105177.
[36] F. Clementi, V. Gazzani, M. Poiani, S. Lenci, Assessment of seismic behaviour of heritage masonry buildings using numerical modelling, Journal of Building Engineering 8 (2016) 29–47, https://doi.org/10.1016/j.jobe.2016.09.005.
[37] P. Kalkbrenner, L. Pelà, C. Sandoval, Multi directional pushover analysis of irregular masonry buildings without box behavior, Eng Struct 201 (2019) 109534, https://doi.org/10.1016/j.engstruct.2019.109534.
[38] G. Milani, M. Valente, Comparative pushover and limit analyses on seven masonry churches damaged by the 2012 Emilia-Romagna (Italy) seismic events: Possibilities of non-linear finite elements compared with pre-assigned failure mechanisms, Eng Fail Anal 47 (2015) (2012) 129–161, https://doi.org/10.1016/j.engfailanal.2014.09.016.
[39] G. Castellazzi, A.M. D'Altri, S. de Miranda, F. Ubertini, An innovative numerical modeling strategy for the structural analysis of historical monumental buildings, Eng Struct 132 (2017) 229–248, https://doi.org/10.1016/j.engstruct.2016.11.032.
[40] S. Degli Abbati, A.M. D'Altri, D. Ottonelli, G. Castellazzi, S. Cattari, S. de Miranda, S. Lagomarsino, Seismic assessment of interacting structural units in complex historic masonry constructions by nonlinear static analyses, Comput Struct 213 (2019) 51–71, https://doi.org/10.1016/j.compstruc.2018.12.001.
[41] F. Micelli, A. Cascardi, Structural assessment and seismic analysis of a 14th century masonry tower, Eng Fail Anal 107 (2020) 104198, https://doi.org/10.1016/j.engfailanal.2019.104198.
[42] F. Peña, P.B. Lourenço, N. Mendes, D.V. Oliveira, Numerical models for the seismic assessment of an old masonry tower, Eng Struct 32 (2010) 1466–1478, https://doi.org/10.1016/j.engstruct.2010.01.027.
[43] P.B. Lourenço, N. Mendes, L.F. Ramos, D.V. Oliveira, Analysis of masonry structures without box behavior, International Journal of Architectural Heritage 5 (2011) 369–382, https://doi.org/10.1080/15583058.2010.528824.
[44] Y. Endo, L. Pelà, P. Roca, Review of different pushover analysis methods applied to masonry buildings and comparison with nonlinear dynamic analysis, J. Earthq. Eng. 21 (2017) 1234–1255, https://doi.org/10.1080/13632469.2016.1210055.
[45] C. Riccio, A. Remus, S. Tezcan, L.C. Silva, G. Milani, R. Perucchio, A macroblock 2D finite element model for assessing the roots of failure of Huaca de la Luna's main pyramid (Peru) under seismic action, Eng Fail Anal 151 (2023) 107417, https://doi.org/10.1016/j.engfailanal.2023.107417.
[46] M. Acito, M. Bocciarelli, C. Chesi, G. Milani, Collapse of the clock tower in Finale Emilia after the Emilia Romagna earthquake sequence: Numerical insight, Eng Struct 72 (2014) (2012) 70–91, https://doi.org/10.1016/j.engstruct.2014.04.026.
[47] E. Nastri, M. Tenore, P. Todisco, Calibration of concrete damaged plasticity materials parameters for tuff masonry types of the Campania area, Eng Struct 283 (2023) 115927, https://doi.org/10.1016/j.engstruct.2023.115927.
[48] A.M. D'Altri, G. Castellazzi, S. de Miranda, A. Tralli, Seismic-induced damage in historical masonry vaults: A case-study in the 2012 Emilia earthquake-stricken area, Journal of Building Engineering 13 (2017) (2012) 224–243, https://doi.org/10.1016/j.jobe.2017.08.005.
[49] M. Schiavoni, E. Giordano, F. Roscini, F. Clementi, Numerical modeling of a majestic masonry structure: A comparison of advanced techniques, Eng Fail Anal 149 (2023) 107293, https://doi.org/10.1016/j.engfailanal.2023.107293.
[50] M. Resta, A. Fiore, P. Monaco, Non-linear finite element analysis of masonry towers by adopting the damage plasticity constitutive model, Adv. Struct. Eng. 16 (2013) 791–803, https://doi.org/10.1260/1369-4332.16.5.791.

[51] M. Valente, G. Milani, Non-linear dynamic and static analyses on eight historical masonry towers in the North-East of Italy, Eng Struct 114 (2016) 241–270, https://doi.org/10.1016/j.engstruct.2016.02.004.
[52] A. De Iasio, P. Wang, J. Scacco, G. Milani, S. Li, Longhu pagoda: Advanced numerical investigations for assessing performance at failure under horizontal loads, Eng Struct 244 (2021) 112715, https://doi.org/10.1016/j.engstruct.2021.112715.
[53] G. Castellazzi, A.M. D'Altri, S. de Miranda, A. Chiozzi, A. Tralli, Numerical insights on the seismic behavior of a nonisolated historical masonry tower, Bull. Earthq. Eng. 16 (2018) 933–961, https://doi.org/10.1007/s10518-017-0231-6.
[54] N. Kumar, M. Barbato, New constitutive model for interface elements in finite-element modeling of masonry, J Eng Mech 145 (2019) 04019022, https://doi.org/10.1061/(asce)em.1943-7889.0001592.
[55] R. Senthivel, P.B. Lourenço, Finite element modelling of deformation characteristics of historical stone masonry shear walls, Eng Struct 31 (2009) 1930–1943, https://doi.org/10.1016/j.engstruct.2009.02.046.
[56] O. AlShawa, D. Liberatore, L. Sorrentino, Combined finite-discrete element model simulations of shake-table tests on a full-scale masonry cross vault, International Journal of Architectural Heritage (2024) 1900–1914, https://doi.org/10.1080/15583058.2024.2317455.
[57] İ. Kocaman, M. Gürbüz, Collapse mechanism of narthex part of historical masonry mosques, Eng Fail Anal 151 (2023) 107387, https://doi.org/10.1016/j.engfailanal.2023.107387.
[58] M. Kujawa, I. Lubowiecka, C. Szymczak, Finite element modelling of a historic church structure in the context of a masonry damage analysis, Eng Fail Anal 107 (2020) 104233, https://doi.org/10.1016/j.engfailanal.2019.104233.
[59] M. Schiavoni, E. Giordano, F. Roscini, F. Clementi, Advanced numerical insights for an effective seismic assessment of historical masonry aggregates, Eng Struct 285 (2023) 115997, https://doi.org/10.1016/j.engstruct.2023.115997.
[60] J. Azevedo, G. Sincraian, J.V. Lemos, Seismic behavior of blocky masonry structures, Earthq. Spectra 16 (2000) 337–365, https://doi.org/10.1193/1.1586116.
[61] J.V. Lemos, A. Campos Costa, Simulation of shake table tests on out-of-plane masonry buildings. Part (V): discrete element approach, International Journal of Architectural Heritage 11 (2017) 117–124, https://doi.org/10.1080/15583058.2016.1237587.
[62] M. Malena, F. Portioli, R. Gagliardo, G. Tomaselli, L. Cascini, G. de Felice, Collapse mechanism analysis of historic masonry structures subjected to lateral loads: A comparison between continuous and discrete models, Comput Struct 220 (2019) 14–31, https://doi.org/10.1016/j.compstruc.2019.04.005.
[63] Z. Zhang, L. Davis, D. Malomo, Distinct Element macro-crack networks for expedited discontinuum seismic analysis of large-scale URM structures, Journal of Building Engineering 97 (2024) 110962, https://doi.org/10.1016/j.jobe.2024.110962.
[64] F. Gobbin, G. de Felice, J.V. Lemos, Numerical procedures for the analysis of collapse mechanisms of masonry structures using discrete element modelling, Eng Struct 246 (2021) 113047, https://doi.org/10.1016/j.engstruct.2021.113047.
[65] R.A. Keys, S.K. Clubley, Establishing a predictive method for blast induced masonry debris distribution using experimental and numerical methods, Eng Fail Anal 82 (2017) 82–91, https://doi.org/10.1016/j.engfailanal.2017.07.017.
[66] D. Malomo, B. Pulatsu, Discontinuum models for the structural and seismic assessment of unreinforced masonry structures: a critical appraisal, Structures 62 (2024) 106108, https://doi.org/10.1016/j.istruc.2024.106108.
[67] R.K. Adhikari, A. Parammal Vatteri, D. D'Ayala, Seismic performance assessment of low-rise unreinforced and confined brick masonry school buildings using the applied element method, Buildings 13 (2023) 159, https://doi.org/10.3390/buildings13010159.
[68] F. Vanin, A. Penna, K. Beyer, A three-dimensional macroelement for modelling the in-plane and out-of-plane response of masonry walls, Earthq Eng Struct Dyn 49 (2020) 1365–1387, https://doi.org/10.1002/eqe.3277.
[69] G. Milani, P.B. Lourenço, A. Tralli, Homogenised limit analysis of masonry walls, Part I: failure surfaces, Comput Struct 84 (2006) 166–180, https://doi.org/10.1016/j.compstruc.2005.09.005.
[70] E. Reccia, A. Cazzani, A. Cecchi, FEM-DEM modeling for out-of-plane loaded masonry panels: a limit analysis approach, The Open Civil Engineering Journal 6 (2012) 231–238, https://doi.org/10.2174/1874149501206010231.
[71] M. Pepe, M. Pingaro, P. Trovalusci, E. Reccia, L. Leonetti, Micromodels for the in-plane failure analysis of masonry walls: Limit analysis, FEM and FEM/DEM Approaches, Frattura Ed Integrita Strutturale 14 (2020) 504–516, https://doi.org/10.3221/IGF-ESIS.51.38.
[72] G. Milani, P. Lourenço, A. Tralli, 3D homogenized limit analysis of masonry buildings under horizontal loads, Eng Struct 29 (2007) 3134–3148, https://doi.org/10.1016/j.engstruct.2007.03.003.
[73] P. Wang, G. Milani, Seismic vulnerability prediction of masonry aggregates: Iterative Finite element Upper Bound limit analysis approximating no tensile resistance, Eng Struct 293 (2023) 116595, https://doi.org/10.1016/j.engstruct.2023.116595.
[74] H.R. Lotfi, P.B. Shing, Interface model applied to fracture of masonry structures, J. Struct. Eng. 120 (1994) 63–80, https://doi.org/10.1061/(asce)0733-9445(1994)120:1(63).
[75] P.B. Lourenço, J.G. Rots, Multisurface interface model for analysis of masonry structures, J Eng Mech 123 (1997) 660–668, https://doi.org/10.1061/(asce)0733-9399(1997)123:7(660).
[76] S. Di Pasquale, New trends in the analysis of masonry structures, Meccanica 27 (1992) 173–184, https://doi.org/10.1007/BF00430043.
[77] M. Lucchesi, C. Padovani, G. Pasquinelli, N. Zani, Masonry constructions: Mechanical models and numerical applications, Lecture Notes in Applied and Computational Mechanics 39 (2008) 1–168.
[78] M. Angelillo, A. Fortunato, A. Montanino, M. Lippiello, Singular stress fields in masonry structures: Derand was right, Meccanica 49 (2014) 1243–1262, https://doi.org/10.1007/s11012-014-9880-6.
[79] L. Cascini, F. Portioli, L. Landolfo, 3D Rigid block micro-modelling of a full-scale unreinforced brick masonry building using mathematical programming, International Journal of Masonry Research and Innovation 1 (2016) 189–206, https://doi.org/10.1504/IJMRI.2016.080426.
[80] Presidente del Consiglio dei Ministri, Direttiva del Presidente del Consiglio dei Ministri 9 febbraio 2011 - Valutazione e riduzione del rischio sismico del patrimonio culturale con riferimento alle Norme tecniche per le costruzioni di cui al D.M. 14/01/2008, Gazzetta Ufficiale Della Repubblica Italiana (2011).
[81] P.X. Candeias, A. Campos Costa, N. Mendes, A.A. Costa, P.B. Lourenço, Experimental assessment of the out-of-plane performance of masonry buildings through shaking table tests, International Journal of Architectural Heritage 11 (2017) 31–58, https://doi.org/10.1080/15583058.2016.1238975.
[82] N. Mendes, A.A. Costa, P.B. Lourenço, R. Bento, K. Beyer, G. de Felice, M. Gams, M.C. Griffith, J.M. Ingham, S. Lagomarsino, J.V. Lemos, D. Liberatore, C. Modena, D.V. Oliveira, A. Penna, L. Sorrentino, Methods and approaches for blind test predictions of out-of-plane behavior of masonry walls: a numerical comparative study, International Journal of Architectural Heritage 11 (2017) 59–71, https://doi.org/10.1080/15583058.2016.1238974.
[83] N. Pingaro, M. Buzzetti, G. Milani, Advanced FE nonlinear numerical modeling to predict historical masonry vaults failure: Assessment of risk collapse for a long span cloister vault heavily loaded at the crown by means of a general-purpose numerical protocol, Engineering Failure Analysis 167 (2025) 109070, https://doi.org/10.1016/j.engfailanal.2024.109070.
[84] G. Neri, M. Rogna, Piano Strutturale Comunale di Piacenza, Relazione Geologico-Sismica (2013).